



The role of purines and chloride channels in the function of the mouse retinal pigment epithelium

Sunna Björg Skarphéðinsdóttir

**Ritgerð til meistaraþráðu í líf-og læknávisindum
Háskóli Íslands
Læknadeild
Heilbrigðisvísindasvið**



HÁSKÓLI ÍSLANDS

Hlutverk þúrinergra viðtaka og klórganga í starfssemi litþekju músa

Sunna Björg Skarphéðinsdóttir

Ritgerð til meistaragráðu í líf- og læknávisindum

Umsjónarkennarar: Sighvatur Sævar Árnason, Þór Eysteinnsson

Meistaránámsnefnd: Haraldur Sigurðsson, Sighvatur Sævar Árnason og Þór Eysteinnsson

Lífeðlisfræðistofnun

Læknadeild

Líf- og læknávisindi

Heilbrigðisvísindasvið Háskóla Íslands Júní 2015

The role of purines in the function of the mouse retinal pigment epithelium

Sunna Björg Skarphéðinsdóttir

Thesis for the degree of Master of Biomedical Science

Supervisors: Sighvatur Sævar Árnason, Þór Eysteinnsson

Masters committee: Haraldur Sigurðsson, Sighvatur Sævar Árnason og Þór Eysteinnsson

Department of Physiology

Faculty of Medicine

Biomedical Science

School of Health Sciences

June 2015

This thesis for a M.Sc. degree in Biomedical Sciences may not be reproduced in any way without the permission of the author.

© Sunna Björg Skarphéðinsdóttir 2015

Printed by Háskólaprent Reykjavík, Iceland 2015

Ágrip

Inngangur: Litþekja augans liggur á milli ljósnema og æðulagi augans. Litþekjufrumurnar gegna því mikilvæga hlutverki að flytja næringarefni frá æðulagi til ljósnema augans og flytja jónir, vatn og úrgangsefnis sömu leið tilbaka. Misræmi í flutningum á vatni yfir litþekjufrumurnar getur leitt til uppsöfnunar á vatni við ljósnema augans í sjónhimnu. Þetta ástand getur auðveldlega valdið niðurbroti sjónhimnunnar og skertra starfsemi hennar en þetta talin vera orsök margra augnsjúkdóma. Margar rannsóknir hafa verið gerðar á jónastreymi um litþekju augans úr rottum, svínum, nautum og mannavef í sérstökum Ussing hólfulum, en aldrei áður í músavef. Rannsóknir hafa sýnt að þúrinergir viðtakar fyrir ATP og UTP geta örvað jónaflæði um litþekjuvef. Fram að þessu hafa klórjónagöng á litþekju augans talin vera grunnur fyrir vatns og jóna flutning frá holhlið að blóðhlið í auganu og niðurstöður margra rannsókna hafa gefið til kynna að klórjónagöng séu staðsett á blóðhlið litþekjunnar í auganu

Markmið: Að rannsaka hversu lífvænleg litþekja í augum músa er í Ussing hólfulum, bæði ræktuð og ferskt litþekja. Einnig að öðlast meiri skilning á hlutverki þúrinergra viðtaka í stjórnun á jónaflæði í augum músa, og mikilvægi klórjónaganga í nettó jónaflutningi um litþekju í augum músa. Það var einnig markmið þessa verkefnis að skapa þekkingargrunn fyrir rannsóknir á litþekju í (knock out) músamódelum.

Aðferðir: Heilbrigðar mýs (C57Bl/6J) voru svæfðar og aflífaðar og litþekjan, ásamt undirliggjandi æðu og hvítu og yfirliggjandi sjónhimnu, var sett í sérhönnuð smágerð þekjulíffæraböð (Ussing-hólf) með 0,031 cm² flatamál á opi, með loftaða (5%CO₂/95%O₂) 38°C Krebs lausn á blóðhlið og sjónuhlið þekjunnar. Spennuþvingunartæki var notað til mælinga á nettó jónastraumi yfir litþekjuna (I_{sc}) í $\mu\text{Amp}/\text{cm}^2$. Á fimm mínútna fresti fór 1 mV púls í gegnum vefinn til þess að meta viðnám vefjarins (TER) í $\text{Ohm}\cdot\text{cm}^2$. Fjöldi músa í tilraunum voru alls 6-8 talsins og hvert efni var í Ussing hólfulum í 30 mínútur alls. Niðurstöður eru sýndar sem meðaltal \pm SEM. Mat á áhrifum inngripa var gert með þöruðu t-testi

Niðurstöðurnar: Litþekjuvefur í augum músa getur lifað í allt að 4-5 klukkustundir í Ussing hólfulum og sýnt áhrif við mismunandi efnum. Þúrinergir viðtakar (bæði P2X og P2Y) höfðu hamlandi áhrif á klórjónastraum litþekjunnar. P2X og P2Y viðtakar juku viðnám litþekjunnar marktækt. Hindrun klórjónaganga sýndi greinileg hamlandi áhrif á jónaflæði. Almennur klórgangablokker (NPPB) hamlaði jónastrauminn eingöngu á holhlið þar sem hann ætti ekki að hafa nein áhrif, þetta var svo staðfest með áhrifum á kalsíum háðum klórganga hamlara (CaCCinh-A01). CFTR klórganga hindrari jók marktækt en tímabundið jónastrauminn. Viðnámið á litþekjuvefnum jókst marktækt með klórganga hömlurum í öllum tilfellum.

Ályktanir: Þúrinergir viðtakar hafa hamlandi áhrif á klór jóna flutning um litþekjuna og örvandi áhrif á viðnám vefjarins. Klórgöng gegna mikilvægu hlutverki við jónaflutning um litþekju í augum músa og fleiri klórgöng virðast vera á holhlið vefjarins en blóðhlið.

Abstract

Introduction: The retinal pigment epithelium (RPE) lies between the photoreceptor outer segments of the retina and the choroid of the eye. The cells of the RPE layer have important role in transporting water and ions from the photoreceptors to the choroid of the eye and in transporting nutrition back the same way. Failure of the water transport can lead to further accumulation of water in the cells of the retina. This can easily cause photoreceptor breakdown and dysfunction that can have severe effects on vision. The function of the short circuit current of RPE cells in the eye has been investigated in Ussing chambers using a variety of animal tissues such as rat, bovine and pig, as well as human, but never before on mouse RPE tissue. Previous research has shown that purinergic receptors can stimulate the short circuit current of the RPE cells. Until now chloride channels have been thought to be the most effective channels to stimulate transport of water molecules from the photoreceptors across the RPE cells to the choroid and several studies have suggested that the chloride channels are situated on the basolateral side of the RPE tissue.

Aims: To establish the viability and feasibility of studying intact murine RPE in cell culture and in vitro in Ussing chambers. To gain understanding of the role of purines in the control of the net transepithelial ion transport of murine RPE. To get a better view on how important chloride channels are in net transepithelial ion transport of murine RPE. To create a theoretical base for research on the RPE in knock-out mouse models.

Methods: Healthy mice (C57B1/6J) were euthanized and the RPE together with the retina, choroid and sclera was mounted in special miniature epithelial chambers with an aperture of 0.031 cm² with normal Krebs on both sides kept at 38°C and aired with 5%CO₂/95%O₂. The tissues were voltage clamped to zero (WPI) to measure the short-circuit current (I_{SC}) in μ Amp/cm². Every 5th minute a 1 mV pulse was passed to estimate the transepithelial resistance (TER) measured in Ohm*cm². The number of mice tested was 6-8 in each series of experiments (one eye per mouse). Each treatment with a substance lasted 30 minutes. The results are presented as a mean \pm SEM. Statistical significance was tested by paired t-test.

Results: The mouse RPE tissue can survive up to 4-5 hours in the Ussing chamber bath and shows responses to drugs. The purinergic receptors (both P2X and P2Y) did decrease the chloride ion current across the mouse RPE. The P2X receptors did cause an increase in the resistance of the mouse RPE significantly, as did the P2Y receptors. A nonspecific chloride channel blocker did only decrease the I_{SC} significantly on the apical side where theoretically it should not affect the tissue; this was then confirmed to be the calcium-activated chloride channel by using a specific antagonist (CaCCinh-A01). A CFTR chloride channel blocker increased the chloride ion current significantly but only transiently. All the chloride channel antagonists used caused significant increases in the transepithelial resistance of the mouse RPE, regardless of their effects on the I_{SC} .

Conclusion: Purinergic receptors decrease the chloride current and increase the transepithelial resistance of the mouse RPE tissue. The chloride channels play a major role in the ionic transport across the mouse RPE tissue. There are more calcium activated chloride channels situated on the apical side than the basolateral side in the mouse RPE tissue.

Acknowledgements

The study presented in this thesis was performed at the Department of Physiology, Faculty of Medicine, University of Iceland. The study on mouse genetics was performed at the Department of Genetics, University of Iceland. I am grateful for all the help and support I had through this research, and I would like to thank sincerely my supervisors, Sighvatur Sævar Árnasson and Þór Eysteinnsson both professors at the Department of Physiology, Faculty of Medicine, School of Health Sciences, University of Iceland and the third member of the master committee, Haraldur Sigurðsson. I would also like to thank Bjarni Agnarsson for taking the time to perform a stained histology on our mice RPE tissue. I would like to thank Hans Guttormur Þormar for endless patience and help with PCR and mutation analysis among other research work. And I would like to thank the staff and coworkers at the Department of Physiology for their assistance and concern, especially Lilja Guðrún Steinsdóttir for her kindness and technical assistance and Anna Guðmunds for all of their help and support. I would also like to thank The Icelandic Research Fund for their great support by a grant for this project. Finally I want to thank my family for endless support and patience throughout this study.

Table of contents

Ágrip	3
Abstract	5
Acknowledgements	7
Table of contents	9
List of figures	11
List of Tables	12
List of abbreviations	13
1 Introduction	15
1.1 Epithelial tissues, function and structure	15
1.2 Epithelial ion transport pathways	16
1.3 The retinal pigment epithelium	17
1.4 Retinal pigment epithelial function	18
1.4.1 Absorption of light	18
1.4.2 RPE transport	18
1.4.3 Transport from the RPE cells to the blood supply:	20
1.4.4 The effects of light stimuli on the RPE	21
1.4.5 Transport from the blood supply to the photoreceptors	21
1.4.6 Secretion of growth factors and cytokines	21
1.5 Eye diseases involving the RPE	22
1.6 Purinergic receptors	24
1.7 Purinergic receptors on the RPE	24
1.8 Chloride channels	26
1.9 Chloride channels on RPE tissue	26
1.9.1 CaCC chloride channels	26
1.9.2 CFTR chloride channels	27
1.9.3 CIC chloride channels	27
2 Aim of study	29
3 Materials and methods	31
3.1 Isolation of primary cell culture of mouse RPE	31
3.2 Ussing chamber technology	31
3.3 Drugs used in the experiments	34
3.4 Drugs used in the experiments	34
3.4.1 Substances for purinergic receptors experiments	34
3.4.2 Substances used in chloride channel experiments	35
3.4.3 Experimental procedure	36
3.4.4 The purinergic receptors experiments	36
3.4.5 The chloride channels experiments	38
3.5 Polymerase Chain reaction (PCR) and Electrophoresis	39
3.6 Data analysis	39
4 Results	41
4.1 Results from RPE cell culturing	41
4.2 Viability of the RPE tissue in Ussing experiments	41
4.3 Purinergic receptors	42

4.3.1	Effects of ATP application	42
4.3.2	The effects of β y-meATP and PPADS	48
4.3.3	The effects of BzATP and A 839977	50
4.3.4	The effects of 2-Thio UTP and PPADS	52
4.4	Chloride channels	54
4.4.1	The effect of NPPB	54
4.4.2	The effects of CaCCinh-A01	60
4.4.3	Results from the CFTR experiments	62
4.5	Results from genotyping mice DNA for Crb1 ^{rd8}	64
5	Discussion	66
5.1	Ussing Experiments on mouse RPE tissue	66
5.2	The role of purinergic receptors in transepithelial ion transport and resistance	66
5.3	The role of chloride channels in transepithelial ion transport and resistance	69
5.4	Limitations of the data	72
5.5	Next steps	73
6	Conclusion	75
	References	77
	Appendix	81

List of figures

Figure 1 Micrograph of the mouse eye.	18
Figure 2 Model of ion transport mechanisms of the RPE tissue.	19
Figure 3 An experiment on single RPE with the calcium activated chloride channel antagonist.....	33
Figure 4 The I_{SC} and TER in normal Krebs.	42
Figure 5 The effects of apical ATP on the I_{SC}	44
Figure 6 The effects of apical ATP on TER.....	45
Figure 7 The effects of basolateral ATP on the I_{SC}	46
Figure 8 The effects of basolateral ATP on TER.	47
Figure 9 The effects of P2X agonist β y-meATP and the P2X and P2Y antagonist PPADS on TER.	48
Figure 10 The effects of P2X agonist β y-meATP and P2X and P2Y antagonist PPADS on TER. .	49
Figure 11 The effects of P2X ₇ agonist BzATP and its antagonist A839977 on the I_{SC}	50
Figure 12 The effects of P2X ₇ agonist BzATP and its antagonist A839977 on TER.	51
Figure 13 The effects of P2Y agonist, 2-thio UPT and its antagonist PPADS on the I_{SC}	52
Figure 14 The effects of P2Y agonist 2-thio UTP and its antagonist PPADS on TER.....	53
Figure 15 The effects of basolateral chloride channel blocker (4 mM) on I_{SC}	54
Figure 16 The effects of basolateral chloride channel blocker NPPB (4 mM) on the TER.....	55
Figure 17 The effects of the apical chloride channel blocker (1 mM) on the on the I_{SC}	56
Figure 18 The effects of apical chloride channel blocker (0,5 and 1 mM) on TER.....	57
Figure 19 The effects of apical chloride channel blocker (4 mM) on the I_{SC}	58
Figure 20 The effects of the apical chloride channel blocker (4 mM) on TER.	59
Figure 21 The effects of the apical calcium activated chloride channel agonist on the I_{SC}	60
Figure 22 The effects of apical calcium activated chloride channel agonist on TER.....	61
Figure 23 The effects of apical CFTR chloride channels blocker on the I_{SC}	62
Figure 24 The effects of apical CFTR chloride channel blocker on TER.	63
Figure 25 Spots seen in the mouse (C57BL6/J) eye tissue.....	64
Figure 26 Agarose gel electrophoresis on amplicons from mutation analysis of the $Crb1^{rd8}$ mutation.	65
Figure 27 Model of ion transport mechanism based on our results.	72

List of Tables

Table 1 Substances used in purinergic receptors experiments and their effects	35
Table 2 The substances used in experiments on chloride channels and their characteristics.	35
Table 3 Information on substances, bath concentrations and tissue numbers in each experiment	36
Table 4 The purinergic series protocol with ATP substance	37
Table 5 The reaction component of the PCR reaction and their volumes.	39

List of abbreviations

AMP	Adenosine monophosphate
ADP	Adenosine diphosphate
ATP	Adenosine triphosphate
AMD	Age related macular degeneration
Ca ²⁺	Calcium ion
cAMP	Cyclic Adenosine Monophosphate
CFTR	Cystic fibroses transmembrane conductance regulator
ERG	Electroretinogram
EOG	Electrooculargram
ER	Endoplasmic reticulum
I _{sc}	Short-circuit current
IP ₃	Inositol-1,4,5-triphosphate
K ⁺	Potassium ion
KCl	Potassium chloride
M	Moles per liter
NKCC2	Na ⁺ /K ⁺ /2Cl cotransporter
NaCl	Sodium chloride
NPPB	5-nitro-2-(3-phenylpropylamino) benzoic acid)
RP	Retinitis Pigmentosa
SEM	Standard Error of Mean
SRS	Subretinal space
TER	Transepithelial resistance
TEP	Transepithelial potential
UDP	Uridine diphosphate
UTP	Uridine triphosphate
VEGF	Vascular endothelial growth factor
μM	Micro moles per liter

1 Introduction

In recent years eye diseases have been studied extensively with respect to the cells of the retina and the retinal pigment epithelium in the eye. Eye diseases like age-related macular degeneration (AMD), retinitis pigmentosa (RP), Stargardt disease, and Best disease all involve degeneration of the photoreceptors of the retina (rods and cones) and can cause loss of vision and blindness. The cause and mechanisms of the degenerations are not yet known but several studies have suggested that abnormal function of the retinal pigment epithelium may be involved in causing this situation (Wimmers et al. 2007). The role of the RPE in transporting ions and water between the subretinal space and the sclera has been studied extensively, and dysfunction in this mechanism has been related to degeneration of the photoreceptors. Purinergic receptors and chloride channels are known to stimulate ion transport over the RPE tissue and dysfunction of chloride transport has been shown to lead to degeneration of the retina (Bosl et al. 2001; Wimmers et al. 2007).

In this introduction I will discuss the main roles of RPE tissue cells and attempt to shed light on the important function of this monolayer with respect to eye diseases. The physiological basis of the short circuit current across the RPE layer will be discussed, and how purinergic receptors and chloride channels affect the short circuit current of the RPE in healthy eye tissue as compared to retinal diseases.

1.1 Epithelial tissues, function and structure

Epithelial tissue is one of four primary tissue types of the body. Such tissue cover the outer surface of the body, the skin, and inner surfaces of the body, such as the lumens of guts, ducts and lungs, and forms glands both exocrine and endocrine (Stevens and Lowe 2005). There are three main factors involved in maintaining the integrity of the epithelia, the basal lamina, intracellular connections attachment and epithelial maintenance, and renewal. Epithelial cells form cohesive sheets of cells and together these sheets form epithelia. Each epithelium is a barrier with specific properties. All epithelia have a basal membrane which anchors the epithelial tissue to its connective tissue underneath (Campochiaro et al. 1986). The basal membrane provides a barrier that restricts the movement of proteins and other large molecules from the underlying connective tissue into the epithelium. The superficial portion of all basal lamina consists of the lamina lucida, a region dominated by glycoproteins and a network of fine microfilaments that lies closer to the epithelium. In most epithelial tissues the basal lamina has a second, deeper layer, called lamina densa. It contains protein fibers that give the basal lamina strength. Attachment between the protein fibers of the lamina lucida and the lamina densa bind the two layers together (Stevens and Lowe 2005).

Some of the important characteristics of the epithelial tissues are cellularity, regeneration, avascularity and polarity. Cellularity makes the epithelial cells bound close together with cell junctions. Most epithelial cells have an extracellular matrix between them but the RPE cells are not separated with extracellular matrix because they are bound together with tight junctions (Silverthorn 2007). Regeneration is an important characteristic for epithelial cells since these are constantly repaired or replaced every time they are damaged. The fact that the epithelial tissues are avascular means they

don't rely directly on blood supply for nutrition and oxygen. Instead they get their nutrition through diffusion from underlying connective tissue through the basolateral membrane or the apical side of the cells (Silverthorn 2007). Epithelial cells are polarized. That means they have an uneven distribution of surfaces that differ in membrane structure and function on the apical and the basolateral side (Marieb and Hoehn 2007).

The main functions of epithelial tissues are protection and transport of ions and water (Stevens and Lowe 2005). They provide physical protection for exposed and internal surfaces of the body from dehydration, destruction and from chemical or biological agents (Silverthorn 2007). Epithelial exocrine glands secrete mucins, enzymes, water and waste products to the apical surface of the individual gland cells while epithelial endocrine glands secrete hormones by exocytosis into the fluid that is surrounded by the cell (Silverthorn 2007). Absorption and secretion take place on the epithelial apical surface where most epithelia have microvilli and the basolateral surface. The epithelial cells in these locations are specialized in transport and cells with microvilli have at least 20 times the surface area of a cell without them. Larger surface area provides a greater ability to absorb and secrete across the membrane (Silverthorn 2007). Epithelial cells transport ions and water molecules transcellularly and by that maintain correct homeostasis and volume of the body.

The classification of epithelial cells is according to the number of cell layers and shapes of cells at the exposed surface. There are two types recognized of epithelial cell layering: simple and stratified, and three types of epithelial cell shapes: squamous, cuboidal and columnar. Simple epithelium has only a single layer of epithelial cells covering the basal lamina, is relatively thin and fragile and cannot provide much mechanical protection. Stratified epithelium has several layers of epithelial cells above the basal lamina and provides more protection than a single epithelium (Marieb and Hoehn 2007).

1.2 Epithelial ion transport pathways

Epithelial tissue cells have highly developed transport pathways for ions and water. Most of epithelial cells in different tissues transport solutes and water across cell membranes in a similar way. Epithelial cells in the kidney tubules, the retinal pigmented epithelium (RPE) and secretory glands are able to transport ion and water molecules transcellularly, i.e. they transport water and ions through the cells forming the tissue. Epithelial cells express the Na/K-ATPase protein that is situated on the basolateral side in all epithelial tissues except the RPE, where the pump is situated on the apical side (Strauss 2005). The transport of sodium, potassium and chloride ions is known to occur in epithelial cells. There are varieties of sodium channels that have been found on epithelial tissues that transport sodium ions through epithelial cells (Wimmers et al. 2007). The sodium (Na^+) ions are transported into epithelial cells on the apical side through Na^+ channels and are pumped out of the cell at the basolateral side by the Na/K-ATPase. Potassium ions are known to be taken up by the Na/K-ATPase on the basolateral side in all epithelial cells besides the RPE and leak out of the epithelial cells through K leakage channels, also situated on the basolateral side of the epithelial tissue. The transport of chloride ions is mediated by ion selective chloride channels that transport chloride in or out of the cells. The Na/K/2Cl (NKCC1) cotransporter is expressed on epithelial cells and transports one Na^+ ,

one K^+ ion and two Cl^- ions into the cells (Wimmers et al. 2007). The transporter is activated and controlled by electrochemical gradients of Na^+ , K^+ and Cl^- ions. In most epithelial cells the water transport is controlled by an osmotic gradient through aquaporin 1 channels (Reichhart and Strauss 2014; Wimmers et al. 2007).

Water transport in epithelial cells in general is thought to be driven either by Na^+ transport from apical side to the basolateral side, chloride ions follow because of the electrical gradient across the cells and the water follows through aquaporin channels because of the osmotic gradient, or from the basolateral side to the apical side the water transport is driven by chloride transport, Na^+ follows because of the electrical gradient across the cells and water is transported because of the osmotic gradient made by the chloride ion transport. This is the opposite to RPE transport where Na^+ is not thought to play any role and the chloride ions are transported from the apical side over to the basolateral side.

1.3 The retinal pigment epithelium

The retinal pigmented epithelium (RPE) is a monolayer of pigmented epithelial cells in the eye. It is located between the blood supply of the choroid and the light-sensitive outer segments of the photoreceptors of the retina (Peterson et al. 1997; Wimmers et al. 2007). The cells of the RPE are hexagonal, connected with tight junction, and contain pigment granules and organelles that digest the front tip of photoreceptors outer segments (Strauss 2005). The apical side of the RPE faces the subretinal space and the photoreceptors and the basolateral side of the RPE contacts the multilayered Bruch's membrane that is attached to the choroid. The tight junctions of the RPE are situated on the lateral surfaces of the cells and in that way the RPE forms a part of the blood/retina barrier (Strauss 2005). The various functions of the RPE are known to be essential for visual function. The main roles of the RPE tissue are absorption of light, epithelial transport, ion buffering, phagocytosis, secretion and immune modulation (Strauss 2005). The importance of these functions of the RPE will be discussed in a greater detail below.

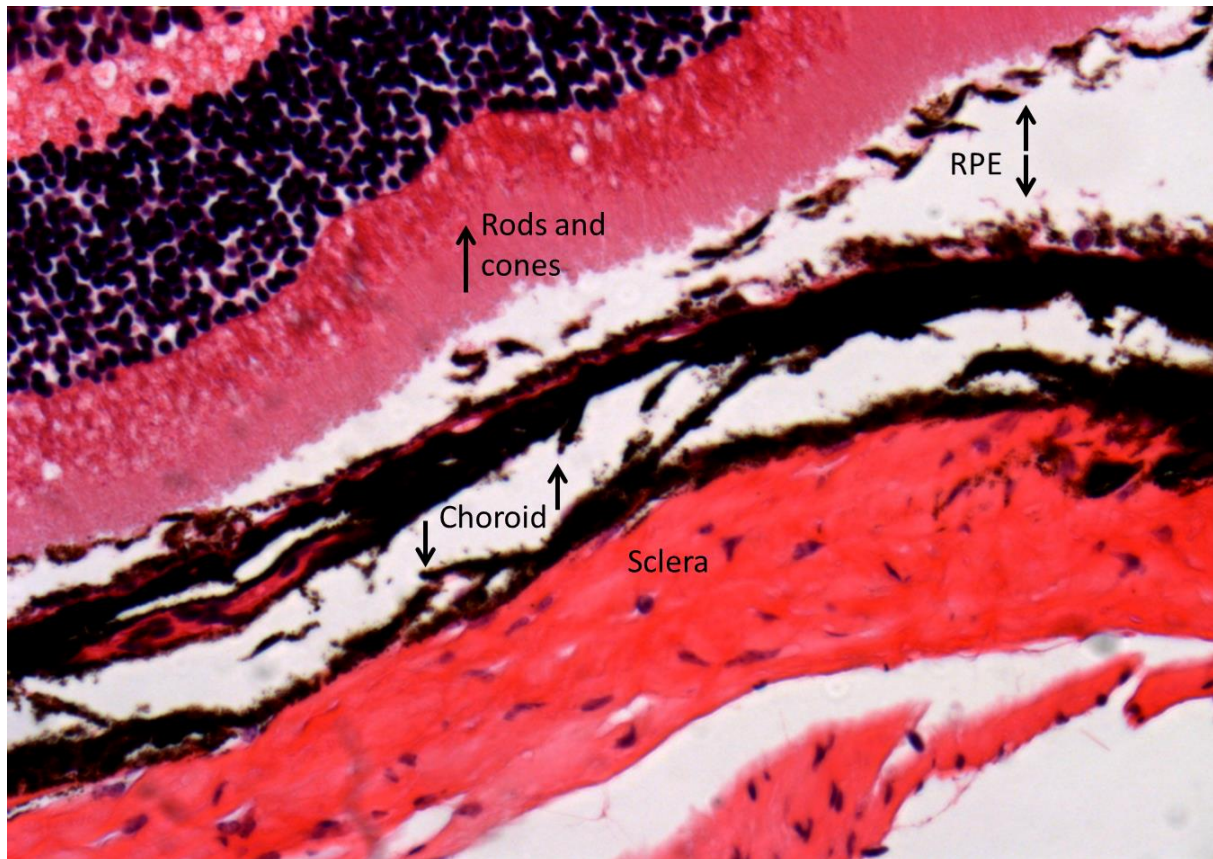


Figure 1 Micrograph of the mouse eye.

The retina layer, RPE, choroid and sclera are shown in the image. The tissue was stained with hematoxylin-eosin.

1.4 Retinal pigment epithelial function

1.4.1 Absorption of light

An important function of the RPE is to clear the damaged outer segments of the photoreceptors by phagocytosis. Photoreceptors need constant repair of their outer segments after being oxidized and damaged while absorbing light from the external environment entering the eye (Beatty et al. 2000). The RPE cells absorb light energy that is focused by the lens onto the retina. The outer retina is exposed to an oxygen rich environment since the blood perfusion from the choriocapillaris is very high and shows 90% O₂ saturation. This oxygen rich environment can lead to photo-oxidation and oxidative damage. The RPE defends the retina for free radicals by renewing the tips of photoreceptor outer segments daily by phagocytosis (Strauss 2005).

1.4.2 RPE transport

Since the RPE tissue transports ions, water and nutrients between layers in the eye it has the structural properties of an ion transporting epithelium (Strauss 2005). Controlling the ionic composition of the cytoplasm of the RPE cells is inevitable because ion transport over the RPE cells maintain ion homeostasis in the subretinal space and the pH value of these cells (Wimmers et al. 2007). A number of studies have been done on animal RPE tissues using Ussing chambers with the voltage clamp technique, and with the patch clamp technique on isolated RPE cells but both

techniques have made it possible to study the cells of epithelia and increase our knowledge of ion channels in this tissue. There are examples of research on ion currents across the cell membranes of isolated RPE cells with the patch clamp technique, where whole cell recordings of chloride currents were performed (Marmorstein et al. 2006).

The RPE tissue has been well characterized in many species such as human, bovine, rat, mouse, frog and pig. The retinal pigmented epithelial tissue of mouse eye has not been experimented on Ussing chambers because of the small size of the tissue.

There are many different mouse models of retinal diseases available, due to mutations in specific genes. Thus it is possible to approach mouse models of several eye diseases and study them in comparison with healthy eye tissue. As examples of such models available now are knockout mice for the *ClC-2* gene (voltage dependent chloride channels), mice that have symptoms comparable to age related macular degeneration and retinitis pigmentosa (RP), and mice models for Best disease. The mice models that are available to study RP are rd10 mice, which have nonfunctional rods and cones (Peng et al. 2014). The mice that are available as a model for Best disease have mutations in the *VMD2* gene (that encode for the bestrophin protein (best-1)) (Marmorstein et al. 2006). The mice available to research Stargardt disease have mutations in the *ABCA4* gene (Peng et al. 2014).

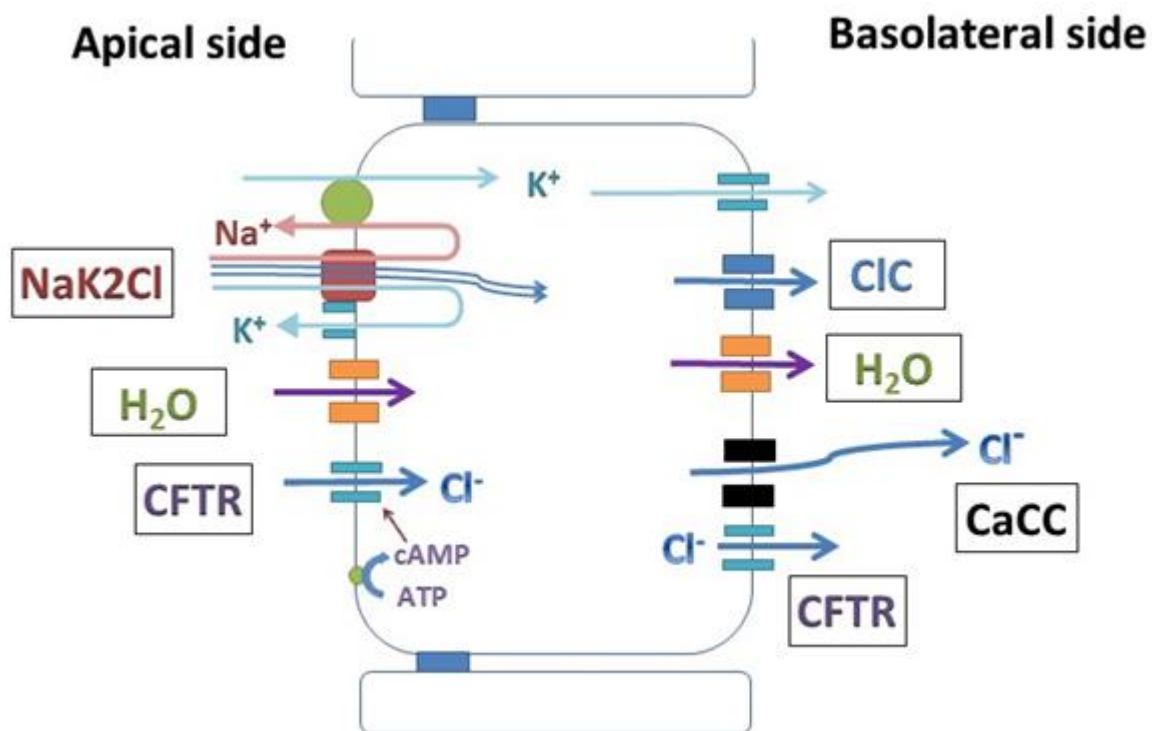


Figure 2 Model of ion transport mechanisms of the RPE tissue.

The figure shows a model of ions transport of the RPE tissue with respect to today's knowledge (Reichhart and Strauss 2014). On the apical side there is a gradient for Na⁺ into the cell provided by the activity of the apical Na/K-ATPase and K⁺ channel. The gradient is used to transport Cl⁻ into the cell via activity of the Na/K/2Cl cotransporter. Cl⁻ leaves the cell on the basolateral side through different chloride channels such as CaCC (calcium activated chloride channel) CFTR (cystic fibrosis transmembrane regulator) and ClC (ClC family chloride channels). cAMP (cyclic adenosine monophosphate) activates the CFTR chloride channels.

1.4.3 Transport from the RPE cells to the blood supply:

The RPE cells mainly transport waste, water and ions across to the choroid of the eye, and show very high transport rate of water, from 1.4 to $11 \mu\text{L} \times \text{cm}^{-2} \times \text{h}^{-1}$ as compared to other epithelial tissue (Edelman and Miller 1991). The transport of water across the RPE cells is mainly driven by the transport of chloride and potassium ions (Strauss 2005). The movement of water occurs mainly by transcellular pathways and it has been shown that transepithelial transport of water is among other processes facilitated by the functional presence of aquaporin 1 channels (Hamann et al. 1998). The transport mechanism of water molecules across the RPE cells to the blood side is extremely important since the photoreceptors have a very high metabolic turnover rate, leading to high production of water in the retina layer every day. Dysfunction of this transport is thought to be the cause of several eye diseases (Strauss 2005). The Na/K-ATPase has an important role in maintaining the ionic homeostasis of the RPE cells as in every other cells of the body. It is situated at the apical side of the RPE cells and by moving two potassium ions into the cell versus 3 sodium ions out of the cell the pump establishes a concentration gradient for sodium ions towards the inside of the cells at the apical side of the RPE. With an inward concentration gradient for Na^+ ions the Na/K/2Cl cotransporter situated on the apical side of the RPE cells is activated. Sodium ions transported into the RPE cells with the cotransporter are transported back to the subretinal space via the Na/K-ATPase (Wimmers et al. 2007). The K^+ ions transported into the RPE cells with the cotransporter recycle back to the subretinal space through K^+ leakage channels situated on the apical side of the RPE membranes (Hughes and Takahira 1996). The chloride ions transported into the RPE cells with the cotransporter are however not transported back to the subretinal space, they are transported over to the choroid with specific Cl^- channels situated on the basolateral side of the RPE (Loewen et al. 2003; Reichhart and Strauss 2014). The result is that of the three ions the cotransporter transports into the RPE cells, the chloride ions are the only ones transported across to the choroid. Until now only a few apical chloride channels have been described and the chloride transport mechanism through the apical membrane of RPE tissues is not fully understood (Reichhart and Strauss 2014; Strauss 2005).

The mechanism of pH homeostasis of the RPE cells is not completely understood, however it seems that raised pH of lysosomes in the RPE cells decreases the function of the lysosomes, which have an important role in breaking down the outer segments of the photoreceptors. A purinergic receptor (P2X_7) seems to induce pH changes in the RPE cells (Guha et al. 2013), but the RPE cells have an important role in eliminating lactic acid from the photoreceptor cells and thereby maintaining acceptable pH values in photoreceptors (Wimmers et al. 2007). There are three main processes that are known to control the intracellular pH of the RPE cells: the $\text{Cl}^-/\text{HCO}_3^-$ exchangers that are situated on the basolateral side of the RPE, and the Na^+/H^+ exchanger and $\text{Na}^+/\text{2HCO}_3^-$ cotransporters that are both situated on the apical side. Some chloride transporters have been shown to be modulated by pH changes (Wimmers et al. 2007). The $\text{Cl}^-/\text{HCO}_3^-$ exchanger transports chloride ions into the RPE cells in exchange for HCO_3^- ions out of the cells, and thus participates by that function in regulating the pH value of the RPE cells. Chloride channels situated on the basolateral side of the RPE cells are activated upon high intracellular acidification (low pH values). This process then stimulates water transport across the basolateral side, which may be important for elimination of water from the retina

during increased metabolic activity (Strauss 2005). The $\text{Cl}^-/\text{HCO}_3^-$ exchanger is at the same time inactivated by the intracellular acidification (Marmorstein et al. 2006).

1.4.4 The effects of light stimuli on the RPE

In response to light stimuli on the eye the cells of the RPE tissue are hyperpolarized when the Fast oscillation (FO) is generated, that is measured with EOG (Arden and Constable 2006). The light peak is a signal mediated by the light peak substance (LPS) which is unknown, but which is supposed to be secreted by the photoreceptors. This substance could possibly be ATP, since ATP can increase intracellular Ca^{2+} and activate chloride channels on the basolateral side of the RPE cells, which then stimulates the net ion transport (Arden and Constable 2006; Marmorstein et al. 2006).

1.4.5 Transport from the blood supply to the photoreceptors

The RPE transports glucose, fat molecules and other nutrients from the blood to the photoreceptors. This transport is essential for the normal function of the photoreceptor cells as they get ω -3 fatty acids to maintain their cell membranes, glucose for energy metabolism, and retinal for the visual cycle of the opsins. To transport glucose the RPE expresses high amounts of glucose transporters, GLUT1 and GLUT3 on both the apical and basolateral membranes (Ban and Rizzolo 2000). The retinal is exchanged between RPE and photoreceptors during the visual cycle in which all-trans-retinol is taken up from photoreceptors and isomerized to 11-cis-retinal, and redelivered to the photoreceptors (Baehr et al. 2003).

1.4.6 Secretion of growth factors and cytokines

It is known that the RPE tissue is able to secrete a variety of different growth factors and immune factors that help maintain the integrity of both the choriocapillaris endothelium and the photoreceptors. One of these growth factors is vascular endothelial growth factor (VEGF) that promotes development of blood vessels in the retina (Eichmann and Simons 2012; Strauss 2005; Wimmers et al. 2007). The RPE cells have been shown to be able to release ATP upon certain situations (Reigada and Mitchell 2005). The cystic fibrosis transmembrane regulator (CFTR) chloride channels are thought to be involved in ATP release from RPE cells that have been shown to be able to auto stimulate the purinergic receptors of the apical membrane of the RPE cells after releasing the substance itself (Reigada and Mitchell 2005). The CFTR channels have been localized on both the apical and the basolateral sides of the RPE cells (Mitchell and Reigada 2008). The RPE cells have been shown to be able to release ATP under conditions such as osmotic stress, rising concentration of glutamate and stimulation of its receptor N-methyl-D-aspartate, stimulation of the NMDA receptors and rising concentration and activation of receptors for basic fibroblast growth factor (bFGF) (Wimmers et al. 2007). The release of ATP often leads to programmed cell death (apoptosis) of the same cell it is released from (Burnstock 2007; Yang et al. 2011).

1.5 Eye diseases involving the RPE

AMD is the most prevalent form of blindness in elderly people worldwide and is thought to be caused by damage in the retina, the RPE cells or its basal layer, the Bruch's membrane. The damage can lead to atrophy of the photoreceptor cells of the retina but the main reason for the early stage of the disease remains unclear (Wimmers et al. 2007; Yang et al. 2011). At the first stage of the disease, which is called the dry form of AMD, lipid molecules accumulate in both the RPE cells and the Bruch's membrane. These lipid molecules are pathological deposits called drusen and are usually situated under the area of macula densa on the RPE layer. When they grow bigger and accumulate further they can easily pressure the macula densa layer and the result is that the area of macula densa can dry and thin out. The macula densa is the part of the retina that is the site for central vision or visual acuity; fine details as viewed during reading or when fixating on something. Patients with AMD often don't have serious loss of vision at the dry form stage of the disease. In the second and more severe stage of the disease blood vessels form in the retina of the eye and can cause a leakage of blood and other fluid. This leakage can cause permanent damage to photo receptors that die and create blind spots in central vision (Ambati and Fowler 2012). This situation can lead to loss of vision. The reason for photoreceptor atrophy in AMD has been attributed to several factors. It has been suggested that RPE cells contribute this disease. As described earlier, one of the main roles of the RPE cells is to phagocyte the outer segments of photoreceptors. Hyper functioning phagocytosis of the photoreceptors by the RPE cells can lead to death of the photoreceptors (Strauss 2005). Lipid accumulation has been shown to increase in the layer of the RPE cells in AMD but that can have serious effects on vision as described above (Zhang et al. 2013). The reason for lipid accumulation in the RPE cells in AMD is not known, but it strongly suggests that the RPE cells are compromised during the development of the disease. At this date there are no effective treatments available to halt the disease process, although there are treatments that slow the progression. Cholesterol decreasing drugs have been used to lower lipid formation in the retina of patients at an early stage of AMD, and antagonists for vascular endothelial growth factor receptors (VEGFR) have been used in the more severe stage to inhibit formation of blood vessels in the retina (Ambati and Fowler 2012).

Retinitis pigmentosa (RP) is an inherited eye disease where either the photoreceptors or the RPE tissue are dysfunctioning. More than 50 mutations in retinal photoreceptors and the retinal pigment epithelium have been shown to cause nonsyndromic RP (Eysteinnsson et al. 2014). The degeneration of the photoreceptors leads at first to night blindness and later in the disease to reduction of visual acuity, loss of central and peripheral vision that causes so called "tunnel vision" (Eysteinnsson et al. 2014; Ferrari et al. 2011). RP can be confirmed with the electroretinogram (ERG) since the ERG decreases is non-recordable in the disease. The ERG is a response from the neural retinal cells and the photoreceptors, with hardly any contribution from the RPE (Marmorstein et al. 2006). The EOG is a measurement of the function of RPE tissue cells and the transepithelial potential across the RPE is an important component of the EOG (Arden and Constable 2006). No transepithelial potential indicates no RPE transport of chloride ions and water from subretinal space to the choroid tissue, that indicates how important the chloride flow across the RPE from the photoreceptors really is. *Crb1*^{rd8} is one of these mutations, and has been localized on chromosome 1

(Crb1). The mutation is a single nucleotide deletion in the *Crb1* gene, which results in a form of retinal degeneration. Clinical appearance is distinct and shows multiple light-colored spots in the fundus of the eye and focal retinal dysplasia and degeneration (Mattapallil et al. 2012). A study of double knockout (DKO) rd8 mice, where the number of photoreceptor terminals and synaptic ribbons were quantified showed retinal lesions with abnormalities in RPE cells, the Bruch's membrane and the photoreceptors (Zhang et al. 2013). The results of the study showed aggregated lipofuscin-like lysosomes in the RPE cells of the DKO (double knockout of *Ccl2*^{-/-} and *Cx3Crb1*^{-/-}) rd8 cells and thickening of the Bruch's membrane compared to C57BL6/N healthy mice (Zhang et al. 2013). In the rd8 mice it was also found that photoreceptor nuclei protrude into the outer retina that result in irregular outer margin of the outer nuclear layer of the photoreceptors (ONL) that is not found in the C57BL6/N mice. The mice with the rd8 mutation showed dislocated and reduced expression of photoreceptor pigments (Zhang et al. 2013). Cones seem to be more vulnerable to damage than rods in the rd8 mutation mouse model (Zhang et al. 2013).

It has been shown that disruption of the chloride channel subtype CIC-2 can lead to degeneration of the RPE (Bosl et al. 2001). A study of mouse models lacking voltage dependent chloride channels CIC-2 (*CIC-2*^{-/-}) found there was almost no transepithelial potential across the RPE cells and severely reduced short circuit current that supports its role in the transport of transepithelial fluid (Bosl et al. 2001; Wimmers et al. 2007). The explanation for nearly no transepithelial potential in CIC-2 knockout mice may be that the CIC-2 channels are not transporting high levels of the Cl⁻ ions across the basolateral membrane and to the choroid. This leads to accumulation of water in the retina in the photoreceptor layer among neurons of the retina in CIC-2 knockout mice. The absence of the chloride transport has been shown to lead to degeneration of photoreceptors (Wimmers et al. 2007).

Another eye disease is juvenile-onset vitelliform macular dystrophy, or Best disease. The cause of the disease is thought to be mutation in the VMD2 gene that codes for the bestrophin-1 protein (Kramer et al. 2000; Wimmers et al. 2007). The bestrophin-1 proteins are thought to be chloride channels situated on the basolateral side of the RPE. Mutations of the VMD2 gene can lead to degeneration of the photoreceptors of the retina, possibly because of RPE's role in transporting chloride ions and water from the retina to the choroid. The disease shares some phenotypic features with AMD, such as abnormal subretinal accumulation of lipofuscin molecules and choroid neovascularization (Kramer et al. 2000; Wimmers et al. 2007). The diagnosis of Best disease in patients is confirmed by the electrooculogram (EOG) since almost all of these patients show reduction in the light-rise of the EOG (Kramer et al. 2000). The mouse model for Best disease is missing the Vmd2 gene (*Vmd2*^{-/-}) and there is a hypothesis that bestrophin-1 is the Cl⁻ channel that generates the light peak, because disturbing the Vmd2 gene causes reduction in the EOG and the Cl⁻ conductance (Marmorstein et al. 2006). The fact that the VMD2 gene is expressed on the RPE tissue suggests the RPE to be the primary site for causing this eye disease.

When the functions and roles of the RPE are taken together it emerges how essential RPE is for healthy eye function. Degeneration of the retina is a frequent cause of severe retinal diseases. Dysfunction of ion and water transport through RPE is likely to cause of the retinal dysfunction (Brady et al. 2012).

1.6 Purinergic receptors

Purinergic receptors (PR) were first defined in 1976 (Burnstock 2007). They are divided into two main types: P1 and P2. The P1 purinergic receptors are activated by adenosine and the P2 purinergic receptors are activated by ATP (adenosine triphosphate), ADP (adenosine diphosphate) and UTP (uridine triphosphate). Purinergic receptors are found in most tissues in the body, including epithelia. Purinergic receptors are known to work in an autocrine and paracrine manner and to be involved in many cellular functions, such as signal transduction, regulation of blood flow, ion transport, cell volume regulation, neural signaling, cell differentiation and cell proliferation (Corriden and Insel 2010).

The P2 purinergic receptors are divided into five subclasses P2X, P2Y, P2Z, P2U and P2T. These receptors have been divided into families of metabotropic P2Y, P2U and P2T and ionotropic P2X and P2Z receptors.

The P2X purinergic receptors have seven subtypes; P2X₁₋₇ which are all ligand-gated nonselective cation channels. They transport Ca²⁺ and Na⁺ ions into cells. The P2Y receptors have eight subtypes, P2Y_{1,2,4-5,6,8-14} which are all metabotropic, meaning that their activation stimulates second messenger pathways inside cells including activation of membrane-bound G protein, which among other pathways can lead to formation of cAMP and phosphorylation of protein kinase A (PKA). They can also activate phospholipase C through G_q-mediated activation leading to production of inositol-1,4,5-triphosphate (IP₃) and release of Ca²⁺ from intracellular stores including the endoplasmic reticulum (ER) (Maminishkis et al. 2002; Taylor et al. 1999).

1.7 Purinergic receptors on the RPE

Purinergic receptors are situated on the apical side in mouse, rat, bovine and human RPE. The P2 receptor subtypes expressed in mouse RPE are P2X and P2Y (Burnstock 2007). In vitro and in vivo studies have shown that the P2Y₂ receptor is expressed in bovine and in fetal human RPE tissue (Maminishkis et al. 2002). The P2Y₁ receptors have been shown to be able to increase the short circuit current across the RPE, and to contribute to transport of ions over the RPE membrane, which supports its presence in the tissue (Corriden and Insel 2010). Results from studies of the purinergic receptor P2X₇ indicate that the receptor is expressed in RPE cells at the apical side and can increase the short circuit current in RPE cells and induce RPE apoptosis in human RPE (Yang et al. 2011). Purinergic receptors have been shown to influence exocrine and endocrine secretion, ion transport and cell apoptosis in RPE cells (Burnstock 2007).

Patch clamp studies, Ussing chamber experiments and research on cultured RPE cells have shown that ATP is one of the activators of purinergic receptors on these cells. Purinergic receptors have been shown to be able to increase growth factor and cytokine release by the RPE tissue. ATP has also been shown to increase influx of Ca²⁺ ions through the P2X₇ receptor into the RPE cells that can lead to activation of cell apoptosis (Wimmers et al. 2007).

Many studies have shown how both P2Y and P2X purinergic receptors can influence ion currents in the RPE. An in vitro study using Ussing chambers of bovine and rat RPE found that there

is an increased transepithelial net fluid transport of approximately 7 $\mu\text{L}/\text{cm}^2$ per hour induced by the P2YR agonist INS37217 (50 μM applied to the apical side on the tissue) (Maminishkis et al. 2002).

Another research on bovine RPE in Ussing chambers found that 100 μM of ATP applied to the apical side of the RPE tissue was able to increase the transepithelial resistance (TER) (Peterson et al. 1997). In the same study intracellular Ca^{2+} was measured with the calcium-sensitive dye fura-2 AM and it was found that ATP (100 μM) increased the intracellular Ca^{2+} levels from 130 to 420 nM. The increased concentration of Ca^{2+} ions inside the cell after ATP application demonstrates that purinergic receptors can possibly increase intracellular Ca^{2+} , and contribute to Ca^{2+} activated signaling pathways inside the cell (Peterson et al. 1997). Cyclopiazonic acid is an inhibitor of Ca^{2+} ATPase in the intracellular storages of cells reticulum was also used and the result with it was a much smaller Ca^{2+} concentration in the cytosol of RPE cells which indicates how much Ca^{2+} is released from the endoplasmic reticulum (ER) via the Ca^{2+} intracellular signaling pathways (Peterson et al. 1997).

Results from patch clamp experiments on rat RPE cells suggests that rat RPE tissue expresses both P2X and P2Y purinoceptors (Ryan et al. 1999). The goal of this work was to investigate the effects of ATP on membrane currents and intracellular calcium concentration. In 62 % of the RPE cells the ATP (100 μM) induced a fast inward non-selective cation current (NCS). The current was insensitive to P2 purinoceptor antagonists PPADS and suramin, but was activated with ATP (100 μM) and UTP (100 μM). The results were that 38 % of the RPE cells showed a biphasic current response to an addition of ATP to the medium: first there was a fast inward current that was then followed by activation of a delayed outward current. The outward current was blocked by Ba^{2+} , an inhibitor of K^+ delayed rectifier channels (Ryan et al. 1999).

In studies where this was shown the researchers demonstrated how RPE cells both of the human ARPE-19 cell line and fresh bovine RPE cells were able to degrade ATP molecules to ADP with the degradative enzymes NTPDase2-3, and eNPPB1-2-3. The ADP can function as an autocrine messenger by binding to different purinergic receptors (Wimmers et al. 2007). The presence of the degenerative enzymes was confirmed with RT-PCR. The work also demonstrated with fluorescence how ATP and UTP molecules increased intracellular Ca^{2+} . These results suggest that extracellular degradation of ATP in the subretinal space can result in production of ADP. This ADP can then stimulate P2Y receptors on the RPE membranes and augment Ca^{2+} signaling in the RPE (Reigada et al. 2005).

Although previous research has shown how purinergic receptors can affect the ion current in rat and bovine RPE, it has not yet been demonstrated in mouse RPE (Ryan et al. 1999). The questions that I wanted to answer in this thesis were if purinergic receptors are expressed in mouse RPE, and if they are, what type of the receptors are expressed and could they affect the ion current of the mouse RPE as in other animal models.

1.8 Chloride channels

Chloride channels are pores that transport chloride ions in and out of cells across cell membranes. They are situated both on the plasma membranes and on intracellular organelles (Jentsch et al. 2002). It is important to transport these ions since they maintain proper volume of cells and take part in setting the cell resting potential, as well as having other important physiological and cellular roles such as pH regulation, organic solute transport, volume homeostasis, cell migration and proliferation (Jentsch et al. 2002). The chloride ions are negatively charged and need to move against their electrical gradient to enter cells since the intracellular space is negatively charged with reference to the extracellular space (Silverthorn 2007). There are at least five classes of mammalian chloride channels, including CaCC (calcium activated chloride channels), CFTR (cystic fibrosis transmembrane conductance regulator), CIC (voltage sensitive Cl^- channels), ligand-gated chloride channels (GABA and glycine) and volume sensitive chloride channels (Jentsch et al. 2002). Some of these channels are activated by change in membrane potential (are voltage dependent) and others need Ca^{2+} or cAMP for their activation. Cl^- channel gating may depend on the transmembrane voltage (in voltage-gated channels), on cell swelling, on the binding of signaling molecules (as in ligand-gated anion channels of postsynaptic membranes), on various ions e.g anions, H^+ (pH), or Ca^{2+} , on the phosphorylation of intracellular residues by various protein kinases, or on the binding or hydrolysis of ATP. Not all Cl^- channels have been identified at the molecular level, but CIC and CFTR channels are well established (Jentsch et al. 2002). The disruption of several Cl^- channels in mice, such as bestrophin and CIC chloride channels results in blindness (Jentsch et al. 2002), as described in chapter 1.5.

1.9 Chloride channels on RPE tissue

Many chloride channel types have been found in RPE tissues of human, bovine, rat and pig. The transport pathway of chloride through these channels is thought to regulate the volume and chemical composition of the subretinal space (Blaug et al. 2003). The main chloride channel types that have been identified in the RPE are cystic fibrosis transmembrane conductance regulator (CFTR) channels, voltage activated anion channels (CIC), the volume activated chloride channels, cAMP activated chloride channels and calcium activated chloride channels (CaCC) (Strauss 2005). The chloride channels have important role in the formation of the light peak of the EOG in response to a long light stimulus. The light induces hyperpolarization of the basolateral membrane of the RPE tissue and by that an increase in chloride conduction there, which induces a light peak in the EOG. EOG is there for a simple and effective way to measure changes in these activities of the RPE tissue of patients (Marmorstein et al. 2006).

1.9.1 CaCC chloride channels

Calcium activated chloride channels (CaCC) are chloride channels that are activated by calcium ions from intracellular stores or extracellular fluid (Wimmers et al. 2007). The calcium activated chloride channels are thought to be situated on the basolateral side of the RPE tissue. The VMD2 protein situated on the basolateral side of the RPE membrane is thought to be CaCC, since studies have

shown they are activated upon intracellular free calcium. CaCC have been suggested to be important for fluid an ion transport across the RPE tissue. CaCC have been shown to be present in mouse RPE with patch clamp measurements (Wimmers et al. 2007). The membrane transient receptor potential channel family (TRP) is calcium conducting ion channels that are activated via second messenger system by $G\alpha_{q11}$. The fact that the P2YR activates $G\alpha_{q11}$ suggests that these receptors might stimulate the TRP. It is a known fact that both epinephrine and ATP can induce intracellular calcium levels that makes these substances potential activators of the CaCC channels on the basolateral side of the RPE tissue (Wimmers et al. 2007)

1.9.2 CFTR chloride channels

The cystic fibrosis transmembrane conductance regulator channel is a protein that is encoded by the CFTR gene, and functions as an ion channel which transports Cl^- ions across epithelial cell membranes. The CFTR channels are cAMP regulated chloride channels (Blaug et al. 2003). The CFTR channels have been identified on the RPE tissue at the apical and basolateral side of the human fetus RPE tissue and on the basolateral side of many RPE animal tissues (Blaug et al. 2003; Wimmers et al. 2007).

Studies have shown that an increase of cAMP in fetal human RPE induces a decrease in basolateral membrane resistance and stimulates the short circuit current, which is thought to be due to stimulated chloride conductance through the CFTR channels (Wimmers et al. 2007). By stimulating the short circuit current the intracellular chloride concentration decreases which can lead to depolarization of these cells. Although data from recent experiments suggests an increase in basolateral conductance, the effects are complex and possibly reflect different transport pathways (Wimmers et al. 2007).

1.9.3 CIC chloride channels

CIC channels are a family of chloride channels that have been shown to be modulated by cAMP which is indispensable for activation of these channels (Wills et al. 2000). These channels have also been shown to be voltage sensitive. The family of ion channels contains 9 transmembrane helices and each protein forms a single pore. The CIC-2, 3 and 5 have been detected at the cultured human fetal RPE cell line RPE 28-SV4 (Wills et al. 2000) and CIC-7 has also been detected in animal RPE cells at the basolateral side (Reigada and Mitchell 2005).

2 Aim of study

The specific aims of the study were:

1. To establish the viability and feasibility of studying intact murine retinal pigment epithelium (RPE) in cell culture and in vitro in Ussing chambers
2. To gain understanding of the role of purines in the control of the net transepithelial ion transport of murine RPE.
3. To get a better view on how important chloride channels are in net transepithelial ion transport of murine RPE.
4. To create a theoretical base for research on the RPE in knock-out mouse models.

3 Materials and methods

3.1 Isolation of primary cell culture of mouse RPE

The purpose of culturing RPE mouse cells was to use the cells for experiments in Ussing chambers, to measure both the short circuit current (I_{sc}) and transepithelial resistance of the cells.

Mice (*Mus musculus*) of the stock C57BL/6/J from Jackson laboratory were euthanized with CO₂ asphyxiation and the carotids were cut to bleed out the animal. Iodine solution was applied around the eye area and both eyes were enucleated and placed in a beaker with aerated Krebs solution at 38°C. All excess tissues around the eye globes were removed and the eyes were washed twice with aerated Krebs solution. The eyes were dissected and the anterior segments removed by cutting around the equator of the ora serrata. The eyecups were incubated for 45 minutes in four-well plate in DMEM/F-12-1 based medium (Gibco-Invitrogen) with 1 % FBS (fetal 1 % bovine serum) and supplemented with 100 U/mL penicillin and 100 µg/ml streptomycin. The retina was removed leaving the RPE, choroid and sclera intact in the eyecup which was then incubated in PBS with 0,25 % trypsin and 2 mM EDTA. The eyecups were transferred to DMEM-F12-10% FBS, and under a dissecting microscope the RPE cells were separated from the choroid. The RPE cells were seeded onto inserts coated with collagen or laminin and were maintained in a 95%O₂/5%CO₂ incubator. The TER was measured once a week with EVOM (Millipore,USA)

3.2 Ussing chamber technology

Laboratory mice C57BL/6J, at 3-12 months of age, female and male, were used in the experiments. The mice were bought from the Jackson Laboratory (USA). The mouse population was bred in the rodent animal facility of the University of Iceland Biomedical Center (BMC). The animals were transferred to the animal facility of the BMC one week before each experiment. One animal at a time was anesthetized with CO₂ (carbon dioxide) in a closed box for 15-20 seconds, and after that a cervical dislocation was performed and the carotid arteries cut. Whiskers were cut short and the eyes were enucleated. Using a 0.45*12 mm needle (Sterican), a hole in the eye globe posterior to the limbus was punctured and using sterilized forceps and dissecting scissors the cornea and both lenses were removed under a dissecting microscope.

First we tried to isolate the RPE from the retina without any success because of how delicate the mouse eye tissue is. We also tried to isolate the sclera from the eye tissue and we were successful with that operation and some of our measurements were performed without the sclera. We tried our best to leave out the optic nerve when applying the tissue to the inserts, but because of the small size of the tissue (3,2 * 3,4 mm) it was very difficult to leave the optic nerve out of the inserts that have an opening size 0.032 cm². Despite this acceptable and stable recordings of the I_{sc} and the TER of the RPE tissue were accomplished.

The retina, RPE, choroid and sclera were mounted as one preparation into EasyMount Ussing chambers (Physiological Instruments, USA) on special inserts with the very small aperture of 0.032 cm². Five mL of a Krebs buffer solution were added to both the apical and basolateral side of the

tissue. The Krebs solution had the following final ion concentration (mmol/L): Na^+ , 138.6; K^+ , 4.6; Ca^{2+} , 2.5; Mg^{2+} , 1.2; Cl^- , 125.1; HCO_3^- , 21.9; PO_4^{2-} , 1.2; SO_4^{2-} , 1.2; glucose, 11.1. The Krebs solution was maintained at temperature of $38 \pm 1^\circ\text{C}$ by a heating circulator (Heto Lab Equipment). The osmolality of this solution was measured to be 295 ± 5 mOsm ($n = 6-8$).

Two pairs of silver chloride (AgCl) electrodes in connection with Agar bridges made in Krebs without glucose were used in the Ussing chamber experiments. One pair was used to measure the transepithelial potential (TEP). The second pair was used to pass a current to clamp the TEP at zero. The clamping and measurements of the resulting short circuit current (I_{SC}) were done by a DVC-1000 Voltage/Current Clamp unit (World Precision Instruments, USA). Furthermore, the DVC-1000 unit was programmed to pass a current causing a 1 mV deflection in the TEP every 4th minute and the resulting deflections in TEP and I_{SC} were used to calculate the transepithelial resistance, TER, by Ohms law. The TEP was measured in millivolts (mV), the I_{SC} in $\mu\text{A}/\text{cm}^2$ and the TER in $\text{Ohms}\cdot\text{cm}^2$. The output from the DVC-1000 unit was digitized by an analog/digital converter unit (ADInstruments, USA), PowerLab 16/30, and the data collected by a data acquisition software, LabChart 7 (ADInstruments, USA).

In each series of experiments a total of 6-8 mice were tested. A total of 60 mice were used in the experiments represents in this project. Approximately 5-10 mice were also tested but we did not manage to use the data from those experiments due to unsuccessful surgery, poor transepithelial potential, transepithelial resistance or short circuit current of the mouse RPE tissue. Only one eye from each mouse was used in each experimental series. After mounting of the RPE tissue into the Ussing chambers, it was allowed to adapt for 30-40 minutes in normal Krebs before the experiment began. Each experiment was divided into three to six 30 minute periods: first a 30 minute control period, then two to four experimental periods of 30 minute each and finally a second control period, when the substances were washed away with a fresh Krebs solution 3-5 times and the I_{SC} and TER recorded for further 30 minutes in normal Krebs. The weight of the mice ranged between 18-28 g depending on age and gender.

An experiment on one RPE with the CaCC antagonist

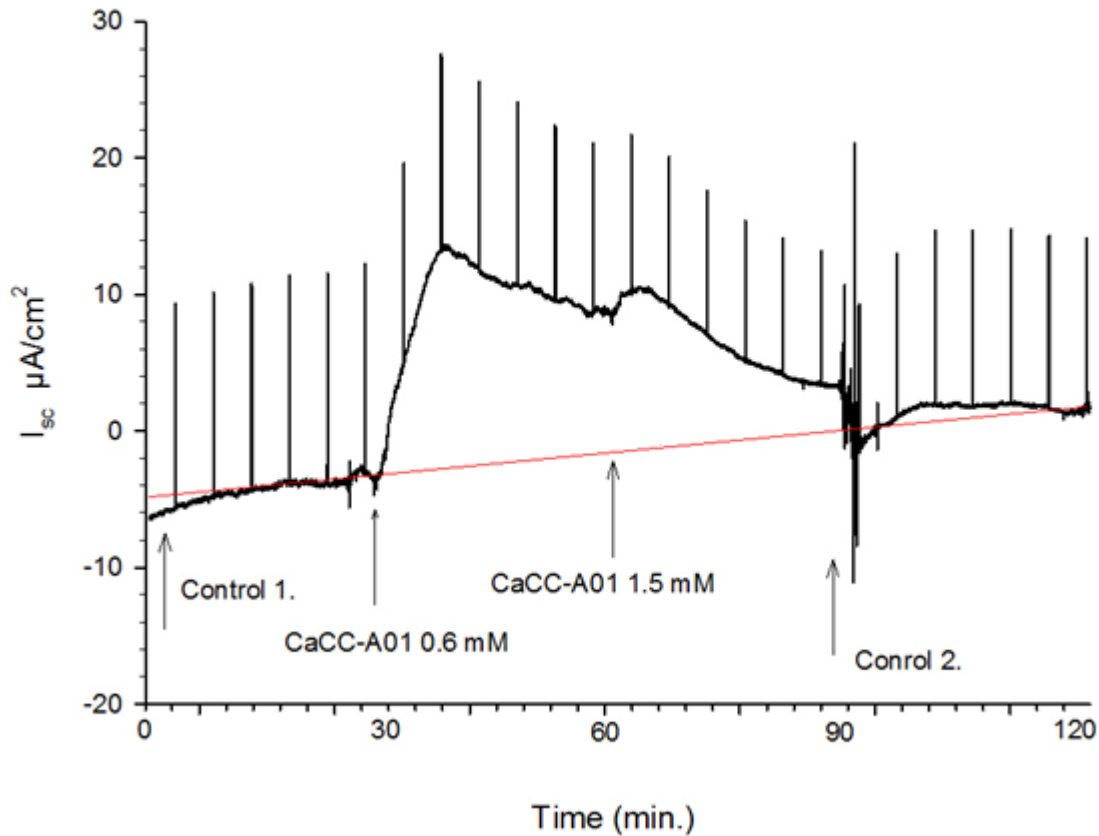


Figure 3 An experiment on single RPE with the calcium activated chloride channel antagonist.

A tracing from one representative experiment recording of the I_{sc} with the calcium activated chloride channel blocker CaCCinh-A01 applied on the apical side of the mouse RPE with the Ussing chamber technology. The changes in the I_{sc} caused by the blocker were highly significant. The I_{sc} decreased and reversed at the higher dose. The ordinate shows the measured value of the I_{sc} from this particular experiment and the abscissa shows the time. The red line indicates the estimated control regression line, calculated with the mean of the I_{sc} measurement 15 minutes before the application of the drug and the first 15 minutes with Control 2 solution in the Ussing chamber bath solution (see section 3.6 for explanation).

3.3 Drugs used in the experiments

Experiments on activation and inhibition of both the purinergic receptors and the chloride channels and their effects on the short-circuit current and transepithelial resistance in RPE tissue were performed with the substances listed below. All substances tested in this project were obtained either from Tocris Bioscience Bristol, UK or Sigma-Aldrich, MO, USA.

A license to use the laboratory animals for the study was granted by the National Laboratory Animal Review Board in Iceland (license number: 0112-0101). The document to confirm the license can be found in appendix A. All experiments were carried out in accordance with the 13. article of regulations number 279/2002 for animal experiments. A diary was kept for all the animal experiments, the care of the animals and cleaning of the animal cages as were performed according to the rules, and once a year a report with review of all animal experiments was turned to the National Laboratory Animal Review Board.

3.4 Drugs used in the experiments

Experiments with activation and inhibition of both the purinergic receptors and the chloride channels and their effects on the short circuit current and transepithelial resistance in RPE tissue were performed with the substances listed below and in tables 1, 2 and 3.

3.4.1 Substances for purinergic receptors experiments

The P2 purinoreceptor agonist ATP (Adenosine 5'-triphosphate disodium salt) (Cat. No.3245) was obtained from Tocris. It is a nonspecific agonist for P2 purinergic receptors that has been widely used in research on purinergic receptors (Ryan et al. 1999).

The P2X purinoreceptor agonist β,γ -Methyleneadenosine 5'-triphosphate disodium salt (Cat. Nr. M7510) was obtained from Sigma-Aldrich. It has been used in experiments on inhibition of extracellular ATP degradation in human and bovine tissue (Reigada et al. 2005).

The P2 purinergic antagonist PPADS (Pyridoxalphosphate-6-azophenyl-2',4'-disulfonic acid tetrasodium salt) (Cat. No. P178) was obtained from Sigma-Aldrich. It is a non-selective P2 purinergic antagonist that blocks P2X₁₋₃ and P2X₅ receptors and all P2Ysubtypes (Ryan et al. 1999).

The P2X₇ agonist BzATP triethylammonium salt (2'(3')-O-(4-Benzoylbenzoyl)adenosine-5'-triphosphate tri(triethylammonium) salt) (Cat. Nr. 3312) was obtained from Tocris. It is a P2X₇ agonist (Burnstock 2007). It has 5-10 fold greater potency than ATP and evokes a higher maximum current. It has partial agonist activity for the P2X₁ and P2Y₁ receptors (Young et al. 2007).

The P2X₇ antagonist A-839977 (1-(2,3-Dichlorophenyl)-N-[[2-(2-pyridinyloxy)phenyl]methyl]-1H-tetrazol-5-amine) (Cat. Nr. 4232) was obtained from Tocris. It is a potent P2X₇ antagonist and

blocks BzATP-evoked calcium influx via recombinant mouse, human and rat epithelial P2X₇ receptors (Jiang 2012).

The P2Y agonist 2-Thio-UTP tetrasodium salt (2-Thiouridine 5'-triphosphate tetrasodium salt) was obtained from Tocris (Cat. Nr.3280). The agonist is a potent and selective agonist for the P2Y_{2,4,6} receptors (El-Tayeb et al. 2006).

Table 1 Substances used in purinergic receptors experiments and their effects

Substance	characteristics
ATP	General P2 purinergic receptor agonist
β,γ-MeATP	P2X purinergic receptor agonist
PPADS	Non-selective P2 purinergic receptor antagonist
BzATP	P2X ₇ purinergic receptor agonist
A 839977	P2X ₇ purinergic receptor antagonist
2-thioUTP	P2Y ₂₋₄₋₆ receptor agonist

3.4.2 Substances used in chloride channel experiments

The chloride channel blocker NPPB (5-Nitro-2-(3-phenylpropylamino) benzoic acid) (Cat. No.0593) was obtained from Tocris. It is a relatively potent inhibitor of chloride conductance activity (Loewen et al. 2003). Clear evidence for a direct effect of NPPB on epithelial chloride channels was found in studies on Cl⁻ fluxes in T₈₄ cell monolayers in Ussing chamber experiments (Keeling et al. 1991), and canine RPE tissue also in Ussing chamber experiment (Kongsuphol et al. 2011; Loewen et al. 2003).

The calcium-activated chloride channel inhibitor CaCCinh-A01 (6-(1,1-Dimethylethyl)-2-[(2-furanylcabonyl)amino]-4,5,6,7-tetrahydrobenzo[*b*]thiophene-3-carboxylic acid) (Cat. No. 4877) was obtained from Tocris. It inhibits the calcium activated chloride current in intestinal cells and has been shown to inhibit chloride ion current in other tissues (De La Fuente et al. 2008)

The chloride channel blocker CFTRinh-172 (4-[[4-Oxo-2-thioxo-3-[3-trifluoromethyl)phenyl]-5-thiazolidinylidene]methyl]benzoic acid) (Cat. No. 3430) was obtained from Tocris. It is voltage-independent, selective CFTR chloride channel blocker that alters channel gating (Reigada and Mitchell 2005).

Table 2 The substances used in experiments on chloride channels and their characteristics.

Substance	Characteristics
NPPB	Chloride channel blocker
CaCCinh-A01	Ca ²⁺ activated chloride channel blocker
CFTRinh-172	CFTR chloride channel blocker

Table 3 Information on substances, bath concentrations and tissue numbers in each experiment

Drug	Molecular weight g/mole	Stock solution mM	Estimated bath concentration mM	Side of tissue	RPE tissues
ATP	551.14	100	1 and 3	Basolateral	6
ATP	551.14	100	1 and 3	Apical	6
β,γ -MeATP	571.15	18	1	Apical	6
BzATP	1018.97	42	0.9 and 1.8	Apical	6
PPADS	5999.3	17	0.1 and 0.5	Apical	8
2-thioUTP	588.13	1,7	0.034 and 0.1	Apical	8
A-839977	413.26	24,2	0.7 and 1.5	Apical	6
NPPB	300.31	100	4	Basolateral	6
NPPB	300.31	100	0.5, 1 and 4	Apical	6
CaCCinh-A01	347.43	28,8	0.58 and 1.2	Apical	6
CFTRinh-172	409.4	20	0.8 and 1.2	Apical	6
Ouabain	584.66	100	0.1	Apical	6

The molecular weight, the stock solutions concentrations and the estimated concentration in the Ussing bath of the drugs used in all the experimental series. The number of tissues used in each experimental series and the side of the tissue tested is also shown in the table.

3.4.3 Experimental procedure

All of the experiments were performed in a similar manner, but with different drugs and doses in each experiment (see section 3.2).

3.4.4 The purinergic receptors experiments

The series of experiments on purinergic receptors were designed to identify the types of purinergic receptors and to examine their effect on the ion current (I_{SC}), transepithelial potential (TEP) and transepithelial potential (TER) in the mouse RPE tissue.

In a series of experiments on the P2 purinergic receptor, first a normal Krebs solution (5 mL) was added to the both sides of the Ussing chambers to obtain control measurements. ATP (1mM) was then added into the Ussing chamber on the apical side, and it remained in the bath for 30 minutes. A second dose of ATP was added to the Ussing chamber bath apically to increase its concentration to 3 mM for 30 minutes. In the end, the Ussing chamber Krebs solution was changed 3-5 times, and normal Krebs was added for 30 minutes.

In the series of experiments with ATP on the basolateral side of the RPE tissue a normal Krebs solution (5 mL) was added to the bath to acquire control measurements. The ATP solution (1mM) was then added in the Ussing chamber on the basolateral side and was kept in the bath for 30 minutes. A second dose of ATP (3 mM) was then added to the Ussing chamber on the basolateral side for 30 minutes. Finally the ATP was removed from the Ussing chambers by washing 3-5 times with normal Krebs on both apical and basolateral sides.

Table 4 The purinergic series protocol with ATP substance

Treatment	RPE side	Time
Control 1	apical + basolateral	1 hour
ATP 1 mM	apical	30 min
ATP 3 mM	apical	30 min
Normal krebs	apical	30 min
ATP 1 mM	basolateral	30 min
ATP 3 mM	basolateral	30 min
Control 2	apical + basolateral	30 min

The ATP series were performed both on the apical and the basolateral side of the RPE tissue. Two doses of ATP substance were applied to the Ussing chamber bath, first 1 mM for half an hour and then 3 mM dose for another half an hour. The bath was then washed with normal Krebs 3-6 times and the same routine repeated to study ATP effects on the basolateral side of the tissue (n=6).

Another experiment to study P2 purinergic receptors were done with the P2X agonist $\beta\gamma$ -meATP and P2X antagonist PPADS (Pyridoxalphosphate-6-azophenyl-2',4'-disulfonic acid tetrasodium salt). Normal Krebs (5 mL) was added to the Ussing bath on both the apical and basolateral side of the RPE tissue and control measurements were made for half an hour. $\beta\gamma$ -meATP (1 mM) was added to the bath solution on the basolateral side of the tissue for 30 minutes. After that, PPADS (0.5 mM) was added to the bath at the basolateral side as well for 30 minutes. At the end, the drugs were removed from the Ussing chambers by washing 3-5 times with normal Krebs both on both the on the apical and basolateral side. The normal Krebs solution was in the bath for 30 minutes for measurement.

The experimental series to test for P2X₇ purinergic receptors was done with the P2X receptor agonist BzATP (2'(3')-O-(4-Benzoylbenzoyl)adenosine-5'-triphosphate tri(triethylammonium) salt) and the P2X₇ antagonist A839977 (1-(2,3-Dichlorophenyl)-N-[[2-(2-pyridinyloxy)phenyl]methyl]-1H-tetrazol-5-amine). Normal Krebs (5 mL) was added to the Ussing bath on both the apical and basolateral side of the RPE tissue and control measurements were observed for half an hour. Then the first dose of the BzATP (941 μ M) was added, and was kept as well in the bath for 30 minutes. The second dose of BzATP was added (1,9 mM) and was also kept in the bath for 30 minutes. The first dose of the P2X₇ antagonist A-839977 (726 μ M) was added to the bath apical side for 30 minutes and second dose of the antagonist (1.5 mM) was added and also kept in bath for 30 minutes. The drugs were then washed away for 3-5 times with normal Krebs solution on both the apical and basolateral side. The normal Krebs solution was in the bath for measurements for 30 minutes after that.

The series of experiments on P2Y purinergic receptors was done with the P2Y receptor agonist 2-ThioUTP (2-Thiouridine 5'-triphosphate tetrasodium salt) and the P2 antagonist PPADS (Pyridoxalphosphate-6-azophenyl-2',4'-disulfonic acid tetrasodium salt). Normal Krebs (5 mL) was added to the Ussing bath on both the apical and basolateral side of the RPE tissue, and control measurements were taken for half an hour. The first dose of the 2-thioUTP (34 μ M) was added to the bath on the apical side and was kept in the bath for 30 minutes. The second dose of 2-ThioUTP was added (102 μ M) and was also kept in the bath for 30 minutes. The first dose of the P2 antagonist

PPADS (102 μ M) was added to the bath apical side for 30 minutes and second dose of the antagonist (510 μ M) was added and also kept in bath for 30 minutes. The bath was washed 3-5 times with normal Krebs solution on both the apical and basolateral side to wash away the drugs. The normal Krebs solution was in the bath for measurement for 30 minutes after that.

3.4.5 The chloride channels experiments

The series of chloride channel experiments was designed to identify what type of chloride channels are situated on either the apical or basolateral side of the RPE tissue and which of them have the greatest influence on the short circuit current (I_{sc}) and transepithelial resistance (TER) of the mouse RPE tissue.

The experimental series to test for chloride channels in general at the basolateral side of the RPE tissue was done with the rather non-specific chloride channel blocker, NPPB (5-Nitro-2-(3-phenylpropylamino) benzoic acid). The first series was with NPPB 4 mM on the basolateral side. First a normal Krebs solution (5 mL) was added to the bath at the apical and basolateral sides and control measurements obtained for one hour. Then NPPB (4 mM) was added to the bath on the basolateral side and kept in the bath for 30 minutes. Then the NPPB was washed away with normal Krebs solution 3-5 times on both the apical and basolateral side, and the normal Krebs solution was kept in the bath for 30 minutes. This was then repeated and the normal Krebs was also kept for 30 minutes.

A series of experiments with lower doses of NPPB was also tested on the apical side with 0.5 and 1 mM doses. First normal Krebs (5 mL) was added to the bath at the apical and basolateral side and control measurements obtained for half an hour. NPPB (0.5 mM) was then added to the bath at the apical side and kept in the bath for 30 minutes. NPPB (1 mM) was added to the bath and also kept for 30 minutes. In the end the NPPB was removed from the bath by washing for 3-5 times with normal Krebs solution that was then and kept in bath for 30 minutes for measurement.

The series of experiments with the blocker NPPB applied to the apical side was also performed the same way as the series with NPPB on the basolateral side, except the drug was applied only on the basolateral side.

A series of experiments for examining the role of calcium-activated chloride channels was done by testing the calcium-activated chloride channel antagonist CaCCinh-A01 (6-(1,1-Dimethylethyl)-2-[(2-furanylcarbonyl)amino]-4,5,6,7-tetrahydrobenzo[*b*]thiophene-3-carboxylic acid). First normal Krebs (5 mL) was added to the bath at the apical and basolateral side and control measurements received for half an hour. The CaCCinh-A01 (0.6 mM) was then added to the bath on the apical side and kept in the bath for 30 minutes. Then a second dose of the agonist (1.2 mM) was added to the apical side of the bath and kept for 30 minutes. The drug was then washed away from the Ussing chamber with normal Krebs for 3-5 times both apical and basolateral side and the normal Krebs was kept in the bath for 30 minutes.

A series of experiments for examining the role of CFTR chloride channels was done using the specific CFTR chloride channel antagonist CFTRinh-172 (4-[[4-Oxo-2-thioxo-3-[3-trifluoromethyl]phenyl]-5-thiazolidinylidene]methyl]benzoic acid). First normal Krebs (5 mL) was added to the bath at the apical and basolateral side and control measurements received for half an hour. The CFTR agonist (0.8 mM) was applied to the bath apical side and kept in the bath for 30 minutes. Then second dose of the agonist (1.2 mM) was added to the apical side of the bath and kept for 30 minutes. The drug was then washed away with normal Krebs for 3-5 times both on the apical and the basolateral side and the normal Krebs was kept in the bath for 30 minutes.

3.5 Polymerase Chain reaction (PCR) and Electrophoresis

PCR was done on the DNA of total 3 of our mice (C57BL/J) to confirm the presence or absence of the rd8 mutation that is a mutation for retinitis pigmentosa (see in chapter 1.5).

Allele specific PCR was done on genomic DNA (see table 5) to confirm the presence or absence of the Crb1^{rd8} mutation using primers: Crb1-Mf1: 5'-GTG AAG AAG ACA GCT ACA GTT CTG ATC; Crb1-Mf2: 5'-GCC CCT GTT TGC ATG GAG GAA ACT TGG AAG ACA GCT ACA GTT CTT CTG; and Crb1-mR 5'- GCC CCA TTT GCA CAC TGA T (Mattapallil et al. 2012). The PCR reaction was as follows: 2 minutes at 94°C and then 49 cycles consisting of 20 second at 94°C, 30 seconds at 50°C and 40 seconds at 72°C, followed by a 7 minutes extension at 72°C. Electrophoresis of the amplicons was performed on a 3 % agarose gel for 22 minutes at a constant 150 volts (Mattapallil et al. 2012). The primers were bought from Biomers.net GmbH.

Table 5 The reaction component of the PCR reaction and their volumes.

Reaction Component	Volume (μl)
ddH ₂ O	5,94
10x PCR Buffer II	1,00
25 mM MgCl ₂	0,34
10 mM dNTP	1,25
10 μM Crb1-mF1	0,20
10 μM Crb1-mF2	0,05
10 μ Crb1-mR	0,17
Taq polymerase	0,05
Tail DNA	1,00
Total Volume	10,0

3.6 Data analysis

In previous studies (Skarphedinsdottir, 2013) it was observed that the I_{SC} and TER of the RPE preparation generally change slowly with time, and it is known that most often these parameters decrease with time, which is possibly due to degeneration of the cells. Therefore, it was decided to have two control periods, one before and one after testing of any substances, and evaluate the effects of the substances by comparing the measured I_{SC} and TER with the calculated I_{SC} and TER according

to a linear regression line drawn between the two control periods. The values used for the regression line were (1) the last 3 points in the Control 1 period, i.e. the last 15 minutes before addition of the first substance, and (2) the last 3 points in the Control 2 period as then we assume that the tissue would have stabilized after the rinsing out of the substances. This method is demonstrated visually in Figure 3.

The difference at each time point between the measured I_{SC} and TER and the values calculated from the slope and intercept of the control regression line was tested by the paired option of the Student's t-Test in Excel 2010 (Microsoft, USA). A value of p below 0.05 was taken as a significant effect by the treatment. The figures were made using Sigma Plot (Version 11; SYSTAT, U.S.A). All results are reported or depicted as means \pm SEM (standard error of mean).

4 Results

4.1 Results from RPE cell culturing

The cells did not manage to survive under these conditions. The problems may lie in the type of inserts used, or they did not manage to live on laminin or collagen and we did not try fibronectin. The TER was measured once a week with EVOM and it decreased with every week until the cells died after 4-6 weeks. The EVOM measurements of TER across the cultured RPE cells was found to range between 0-140 Ohms.

4.2 Viability of the RPE tissue in Ussing experiments

To study the viability, feasibility and the stability of the RPE mouse tissue preparation we did an experimental series with normal Krebs only in the Ussing chamber for 2 ½ hour. We took measurements of the short circuit current (I_{SC}) and the transepithelial resistance (TER), depicted in Figure 3. The results indicated that the tissue was very stable and viable in the Ussing chamber for more than 3 hours. The short circuit current did not change and only a non-significant change was observed in the TER after a fresh Krebs solution exchange. At the end of the experiment the Na/K-ATPase inhibitor ouabain (1 mM) was added to the apical bath solution and its effect showed that the tissue was still alive, as there was a typical increase in I_{SC} and then a decrease towards zero, with a simultaneous increase in TER. Although both I_{SC} and TER showed stable measurements in the beginning of most experiments this was not always the case. Because of this we decided to calculate a control regression line between the two Control periods (the last 15 minutes of Control 1 measurements and last 15 minutes in Control 2 measurements) and compare the measured I_{SC} and the TER to the regression line that lies between those two periods. That was found to be an excellent solution since the Control 1 measurements showed in some of the experiments an unstable recordings for the I_{SC} (see figures 8,12, 22) and for TER (see figures 9,11). Washing out the drugs was not always effective as can be seen in figures 19 and 20.

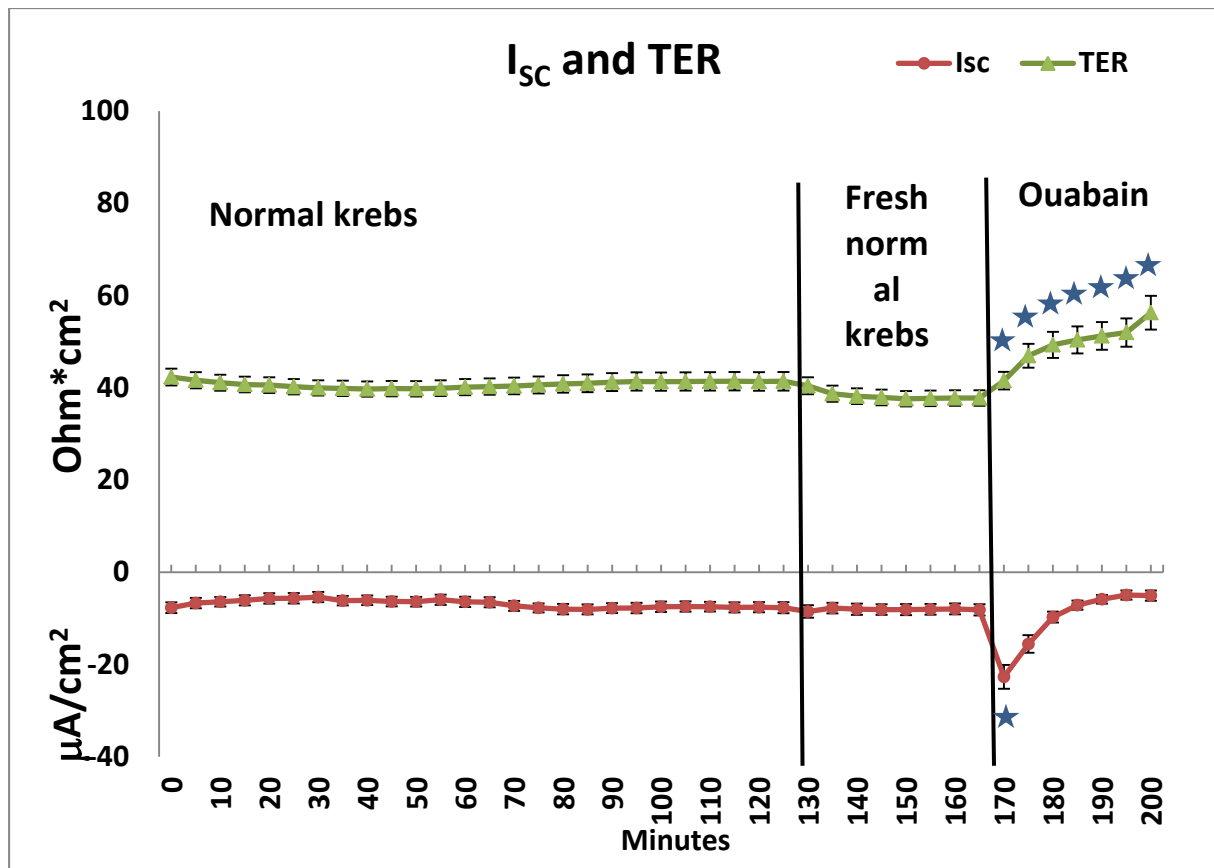


Figure 4 The I_{SC} and TER in normal Krebs.

The figure shows the I_{SC} and TER of a control RPE tissue preparation with normal Krebs for 165 minutes. At 130th minute the Krebs was exchanged with a fresh Krebs solution. At the end of the experiment, the Na/K-ATPase blocker ouabain was added to the apical side (n=6).

4.3 Purinergic receptors

4.3.1 Effects of ATP application

Both apical and basolateral ATP (Adenosine 5'-triphosphate disodium salt) (1-3 mM) caused significant effects on the I_{SC} and TER of the mouse RPE tissue (see figure 5).

The effects of apical ATP on the I_{sc}

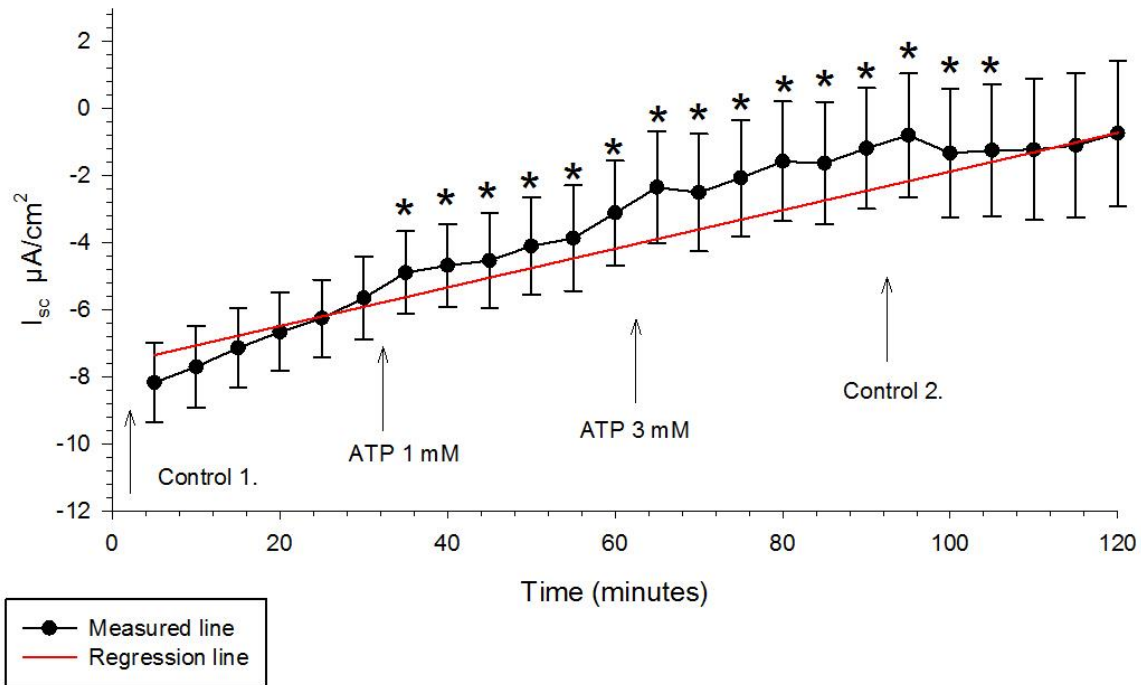


Figure 5 The effects of apical ATP on the I_{sc} .

The figure shows the changes in the I_{sc} with ATP applied to the apical side in the Ussing chamber. The ordinate shows the measured value of the I_{sc} in $\mu\text{A}/\text{cm}^2$ and the abscissa shows the time of the drugs in the bath solution in the Ussing chamber ($n=6$). The red line is the control regression line calculated between the last three I_{sc} measurements of each of the two control periods. The stars indicate a statistical significant difference of the measured I_{sc} compared to the control regression line at each time by paired t-tests.

The I_{sc} decreased significantly with apical ATP application. The I_{sc} decreased from $-5.65 \pm 1,2 \mu\text{A}/\text{cm}^2$ average from the last 5 minutes of Control 1 measurements to $-3,12 \pm 1,6 \mu\text{A}/\text{cm}^2$ after 30 minutes with 1 mM ATP on the apical side in the Ussing chamber. The I_{sc} decreased further to $-1.2 \pm 1,8 \mu\text{A}/\text{cm}^2$ after 30 minutes with apical 3 mM ATP. As described in chapter 3.6, by using a control regression line to compare with measured I_{sc} values, we did exclude the possibility that significant differences in the I_{sc} measurements were a result of the time factor due to e.g. degeneration of the tissue or other unknown factors.

The change in the I_{sc} by both doses of ATP was statistically significant compared to the control regression line ($p=0,003$). The change in I_{sc} caused by a fresh Krebs solution in the Control 2 period indicates that the drug was washed away from the mouse RPE tissue cells.

The effects of apical ATP on TER

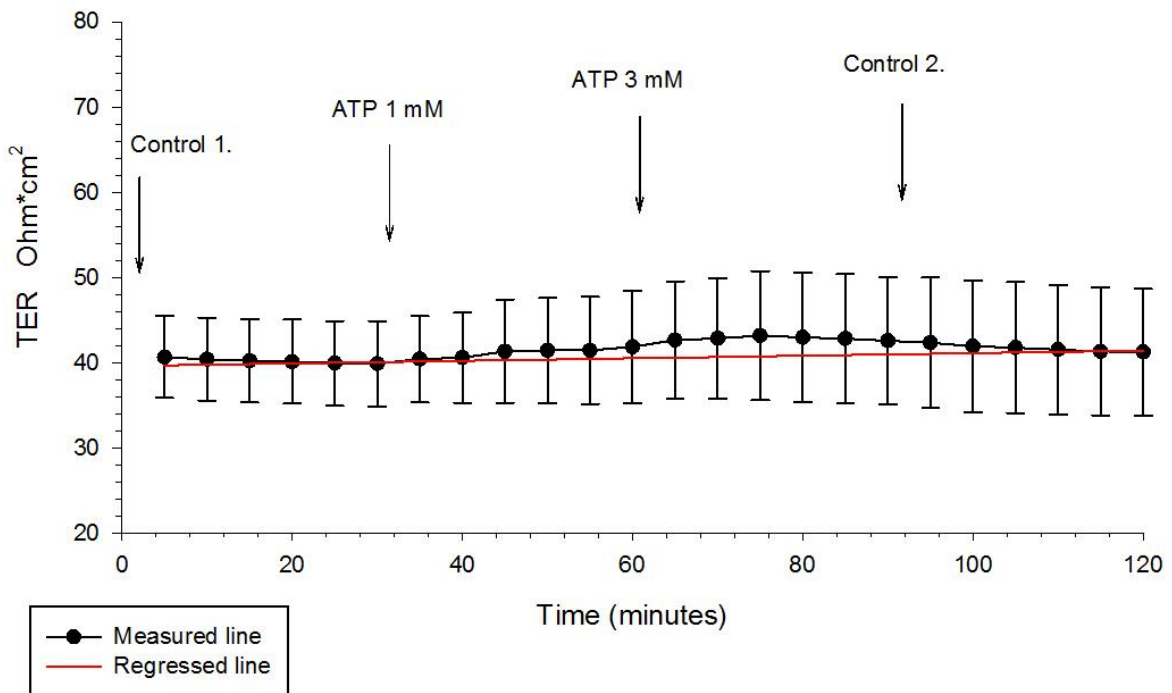


Figure 6 The effects of apical ATP on TER.

The figure shows the changes of the TER with the apical ATP substance in the Ussing chamber bath (n=6). The ordinate shows the measured value of the TER and the abscissa shows the time of the drugs in the bath solution in the Ussing chamber (n=6). The red line is the control regression line calculated between the last three TER measurements of each of the two control periods. The stars indicate a statistical significant difference of the measured TER compared to the control regression line at each time by paired t-tests.

The transepithelial resistance of the RPE mouse tissue did not change significantly with either 1 mM or 3 mM ATP applied to the apical side after 30 minutes of each dose, in comparison to the control regression line. The TER changed from a mean of $39,8 \pm 5$ to a mean of $41,8 \pm 6,6$ Ohm*cm² with the smaller dose (1 mM) of ATP for 30 minutes in the bath solution and to $43,1 \pm 7,6$ Ohm*cm² with the higher dose (3 mM) of ATP in the bath solution for another 30 minutes ($p \leq 0.05$).

The effects of basolateral ATP on I_{sc}

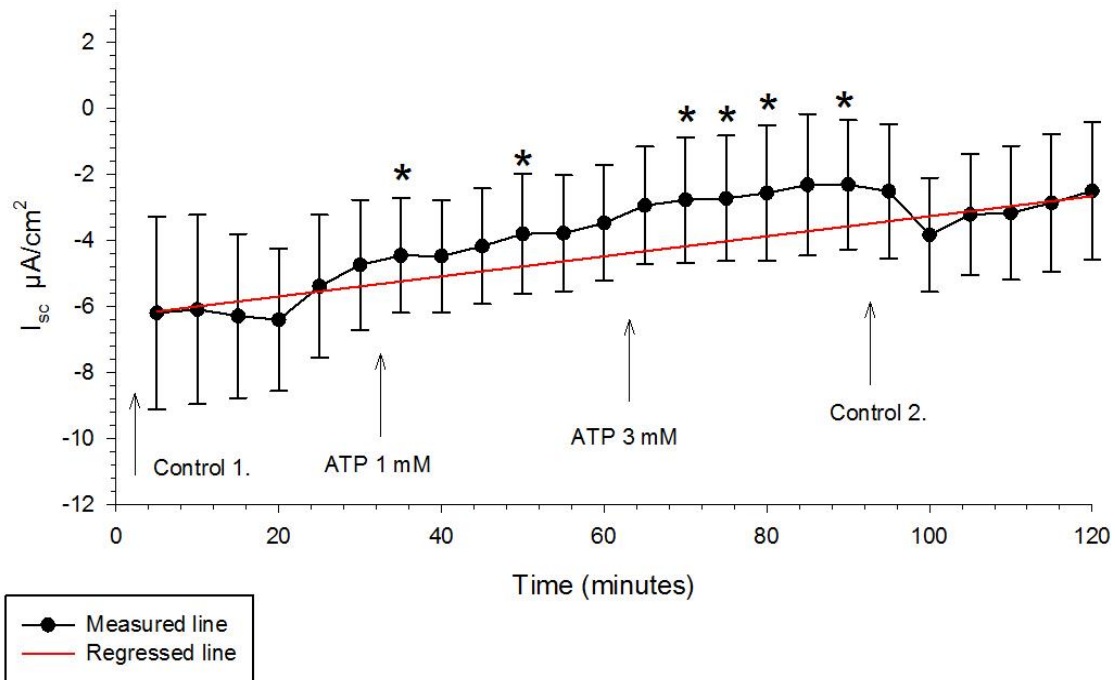


Figure 7 The effects of basolateral ATP on the I_{sc} .

The figure shows the change in the I_{sc} with ATP applied to the basolateral side of the mouse RPE tissue. The ordinate shows the measured value of the I_{sc} and the abscissa shows the time of the drugs in the bath solution in the Ussing chamber ($n=6$). The red line is the control regression line calculated between the last three I_{sc} measurements of each of the two control periods. The stars indicate a statistical significant difference of the measured I_{sc} compared to the control regression line at each time by paired t-tests.

The short circuit current did show a significant decrease when 1-3 mM ATP was applied to the basolateral side. After 30 minutes with the larger dose of ATP (3 mM) in the bath the I_{sc} decreased significantly in comparison to the regression line ($p = 0.03$). The I_{sc} changed from a mean of $-4,7 \pm 2 \mu A/cm^2$ during the last 5 minutes of the Control 1 measurements to $-2,3 \pm 2 \mu A/cm^2$ after 30 minutes with ATP 3 mM dose in the bath. The ATP seemed to be washed from the RPE tissue cells with the normal Krebs solution at the end of the experiment, since the switch to normal Krebs did increase the I_{sc} again after the decrease caused by basolateral ATP.

The effects of basolateral ATP on TER

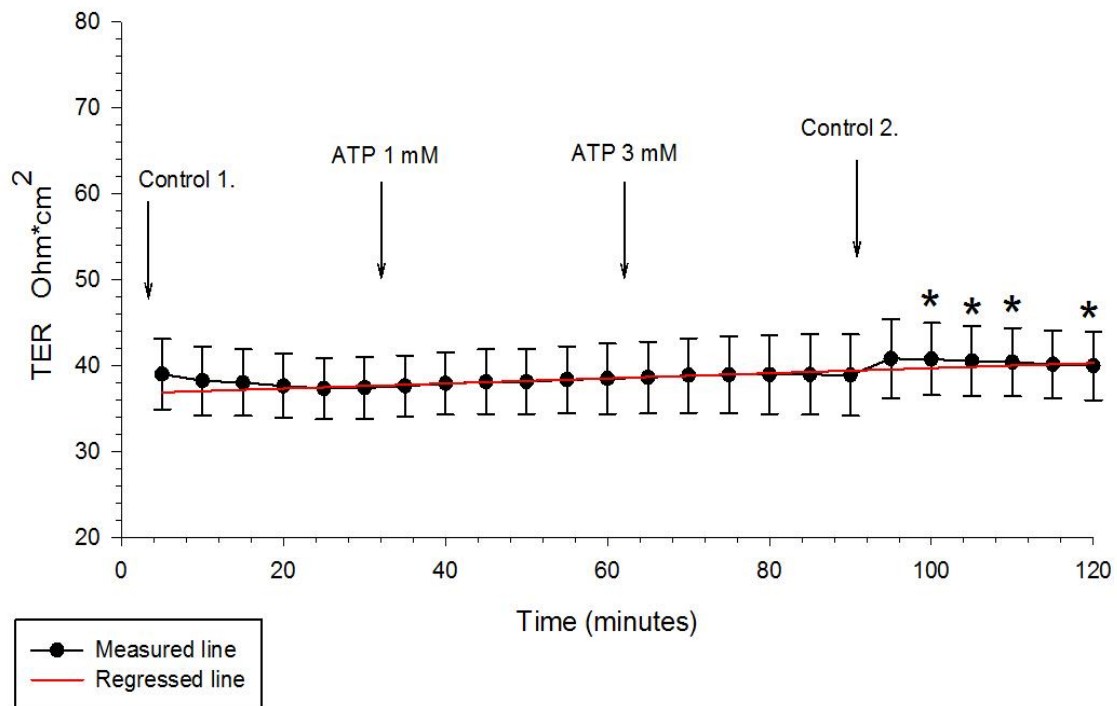


Figure 8 The effects of basolateral ATP on TER.

The figure shows the change in the transepithelial resistance with the basolateral ATP of the RPE mouse tissue. The TER did not change significantly with the substance neither with the lower or higher dose. The ordinate shows the measured value of the TER and the abscissa shows the time of the drugs in the bath solution in the Ussing chamber (n=6). The red line is the control regression line calculated between the last three TER measurements of each of the two control periods. The stars indicate a statistical significant difference of the measured TER compared to the control regression line at each time by paired t-tests.

The transepithelial resistance did not change significantly with ATP (1 and 3 mM) in the basolateral bath solution for 30 minutes with each dose. The TER increased from a mean of $38,9 \pm 4,7 \text{ Ohm*cm}^2$ during the last 5 minutes of basolateral ATP (3 mM) to $40 \pm 4 \text{ Ohm*cm}^2$ for the next 30 minutes with Control 2 measurements. These small but significant effects might indicate that the ATP was perhaps affecting the TER slightly when in the Ussing chamber.

4.3.2 The effects of $\beta\gamma$ -meATP and PPADS

The general P2X agonist $\beta\gamma$ -meATP (1002 μM) induced no significant change in the short circuit current during the 30 minute period of its presence in the Ussing chamber bath on the apical side. The addition of its antagonist PPADS (502 μM) also did not have a significant influence on the ion current (see figure 9)

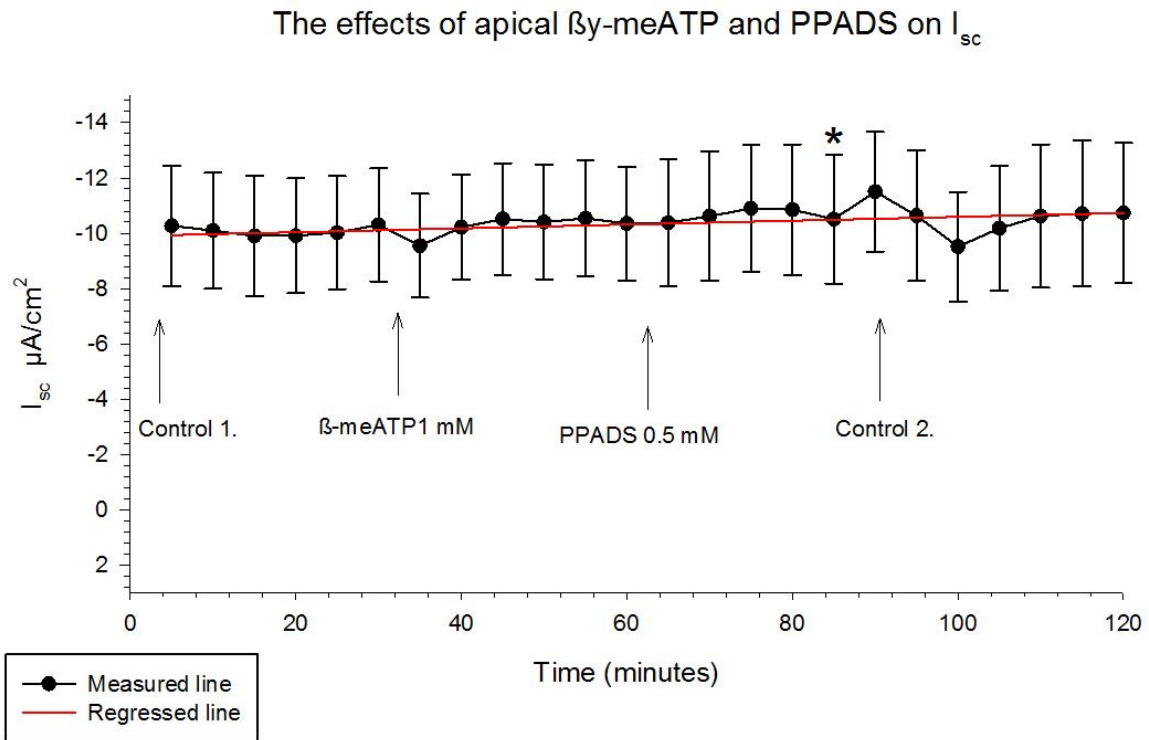


Figure 9 The effects of P2X agonist $\beta\gamma$ -meATP and the P2X and P2Y antagonist PPADS on TER. The figure shows the change in the I_{sc} with $\beta\gamma$ -meATP and PPADS in the bath solution. The ordinate shows the measured value of the I_{sc} and the abscissa shows the time of the drugs in the bath solution in the Ussing chamber ($n=6$). The red line is the control regression line calculated between the last three I_{sc} measurements of each of the two control periods. The stars indicate a statistical significant difference of the measured I_{sc} compared to the control regression line at each time by paired t-tests.

The transepithelial resistance did increase significantly after application of both $\beta\gamma$ -meATP and PPADS in the Ussing chamber bath solution. After 30 minutes with $\beta\gamma$ -meATP in the bath solution the TER changed from a mean of $47,2 \pm 6,1$ to $57,1 \pm 9,5 \text{ Ohm}\cdot\text{cm}^2$ and after 30 minutes with PPADS in the bath solution the TER was unchanged at $57,8 \pm 9,1 \text{ Ohm}\cdot\text{cm}^2$. $\beta\gamma$ -meATP caused significant increase in TER compared to the estimated regression line ($p=0.03$) during the whole 30 minute period. The PPADS did not cause a further significant increase in TER). The change to normal Krebs in the Control 2 period did wash away the drugs from the RPE tissue since the TER decreased again after the increase from $\beta\gamma$ -meATP and PPADS in the bath solution to levels similar to those of Control 1.

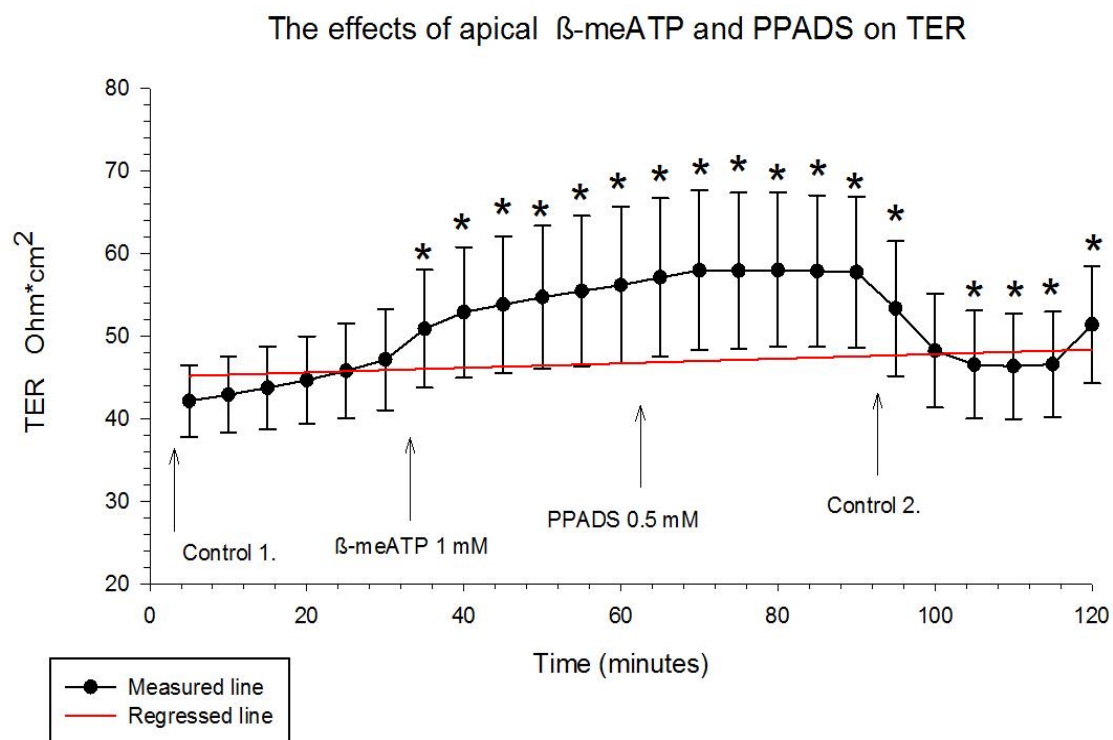


Figure 10 The effects of P2X agonist $\beta\gamma$ -meATP and P2X and P2Y antagonist PPADS on TER.

The figure shows the change in the transepithelial resistance with the $\beta\gamma$ -meATP and PPADS in the Ussing chamber. The ordinate shows the measured value of the TER and the abscissa shows the time of the drugs in the bath solution in the Ussing chamber ($n=6$). The red line is the control regression line calculated between the last three TER measurements of each of the two control periods. The stars indicate a statistical significant difference of the measured TER compared to the control regression line at each time by paired t-tests.

4.3.3 The effects of BzATP and A 839977

The smaller dose of the specific P2X₇ agonist BzATP (941 μ M) caused a significant decrease in the I_{SC} (see figure 11). The addition of the second dose of BzATP (1,8 mM) did not cause any significant change in the I_{SC} during 30 minutes of measurement. The addition of the antagonist for P2X₇, A 839977 did show a significant change in the I_{SC} , but only with the larger dose (1,5 mM) of the antagonist. Changing the bath solution to a fresh normal Krebs solution for the last thirty minutes of the experiment caused a significant decrease in the I_{SC} .

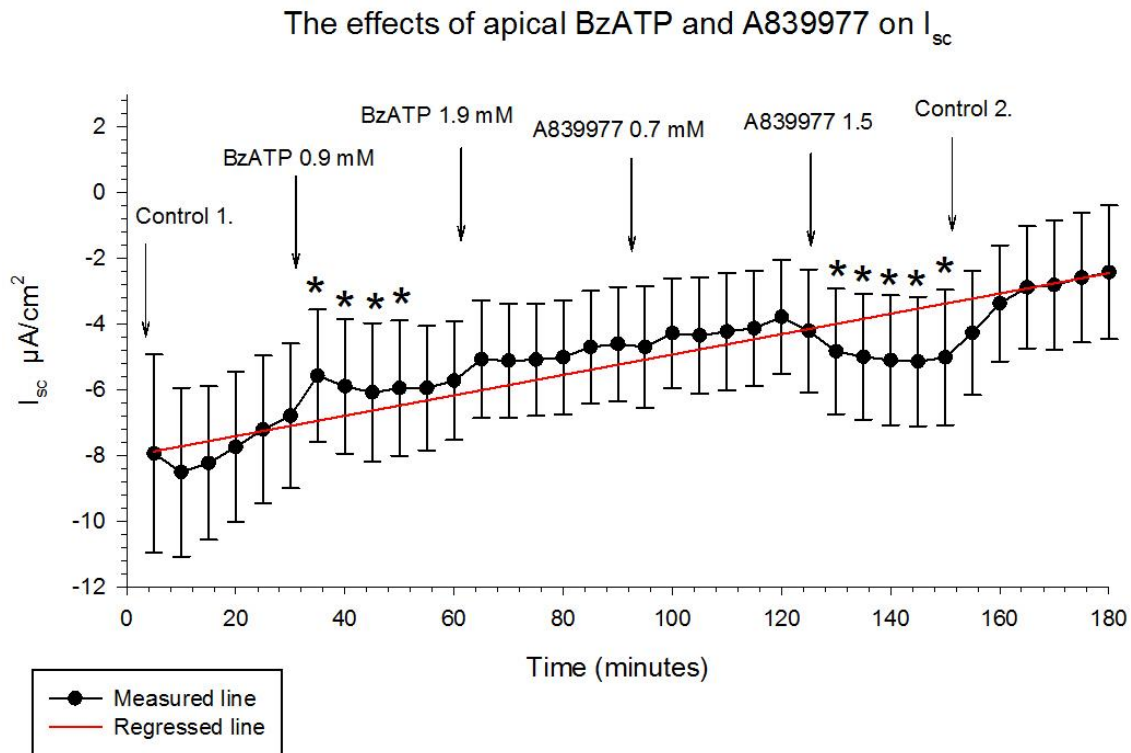


Figure 11 The effects of P2X₇ agonist BzATP and its antagonist A839977 on the I_{SC} .

The figure shows the changes when two different doses of the apical BzATP and A839977 in the Ussing chamber bath solution. The ordinate shows the measured value of the I_{SC} and the abscissa shows the time of the drugs in the bath solution in the Ussing chamber ($n=6$). The red line is the control regression line calculated between the last three I_{SC} measurements of each of the two control periods. The stars indicate a statistical significant difference of the measured I_{SC} compared to the control regression line at each time by paired t-tests.

The TER did increase gradually following application of BzATP into the bath solution, but did not cause a significant change in the TER compared to the control regression line except for the last 5-10 minutes in the Ussing chamber with the higher dose of the agonist (1,9 mM). The increase was significant as compared to the control regression line with both of the doses of the P2X₇ antagonist A839977 (0,7 and 1,5 mM).

It appears that the washing of the drug from the RPE tissue with normal Krebs at the end of the experiment was accomplished since the TER decreased again after the increase with both of the drugs in the bath solution. The TER decreased to $71,1 \pm 16 \text{ Ohm} \cdot \text{cm}^2$ after 30 minutes of control 2 measurements from $90,5 \pm 21,5 \text{ Ohm} \cdot \text{cm}^2$ after 30 minutes with the higher dose of the P2X₇ antagonist A839977.

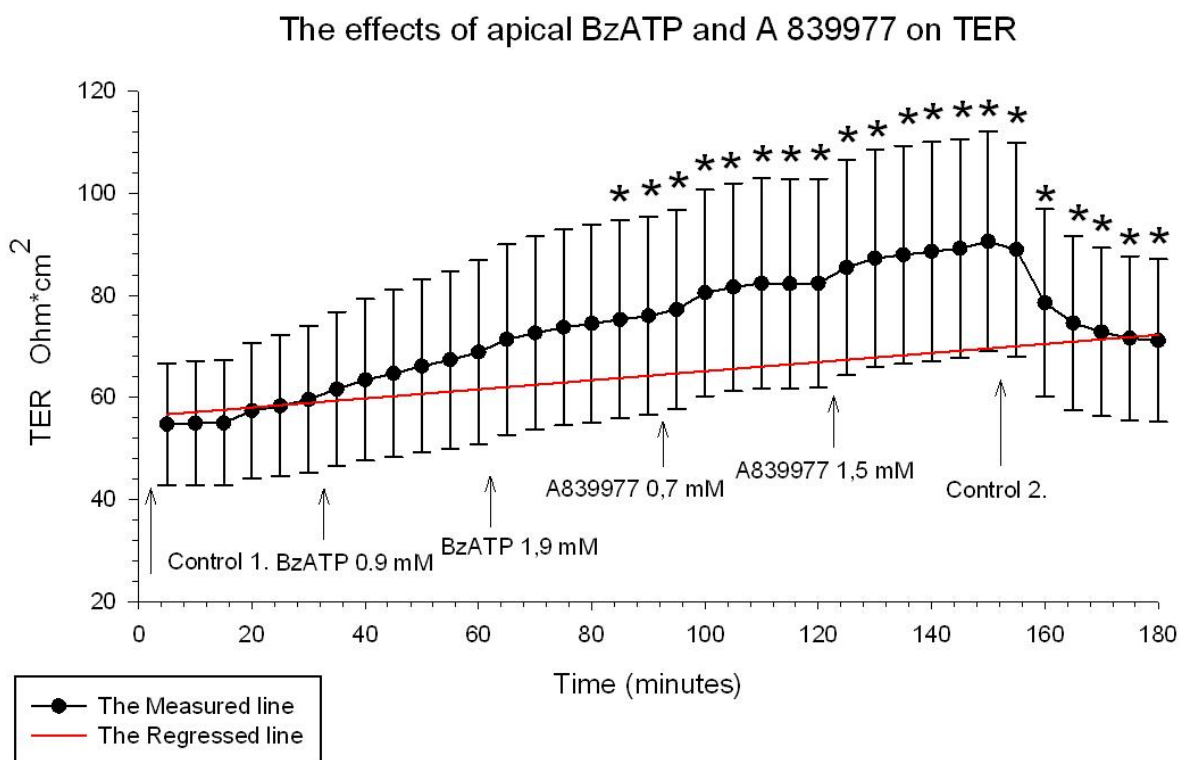


Figure 12 The effects of P2X₇ agonist BzATP and its antagonist A839977 on TER.

The figure shows the change in the transepithelial resistance of the RPE mouse tissue with the P2X₇ agonist BzATP and the nonspecific antagonist A 839977 of P2X and P2Y purinergic channels. The ordinate shows the measured value of the TER and the abscissa shows the time of the drugs in the bath solution in the Ussing chamber (n=6). The red line is the control regression line calculated between the last three TER measurements of each of the two control periods. The stars indicate a statistical significant difference of the measured TER compared to the control regression line at each time by paired t-tests.

4.3.4 The effects of 2-Thio UTP and PPADS

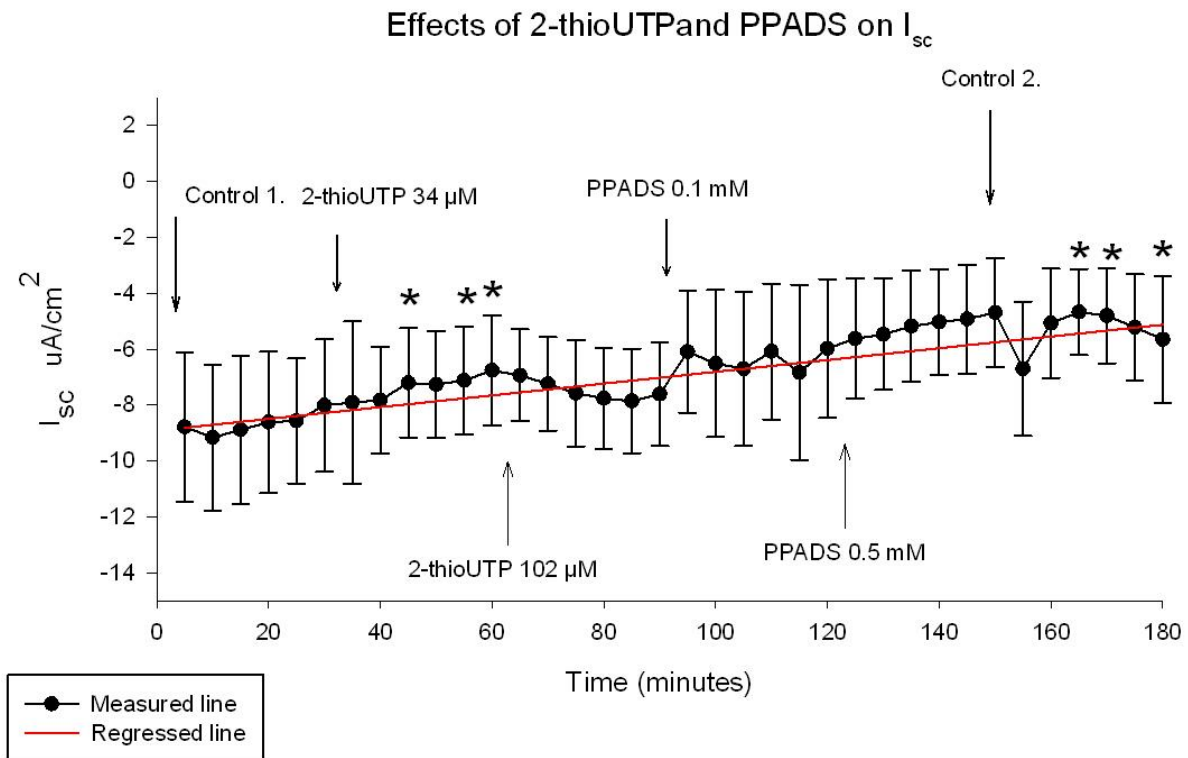


Figure 13 The effects of P2Y agonist, 2-thio UPT and its antagonist PPADS on the I_{sc} .

The figure shows the changes in I_{sc} with the P2Y agonist 2-thio UTP and the P2 antagonist PPADS in the bath solution. The ordinate shows the measured value of the I_{sc} and the abscissa shows the time of the drugs in the bath solution in the Ussing chamber ($n=6$). The red line is the control regression line calculated between the last three I_{sc} measurements of each of the two control periods. The stars indicate a statistical significant difference of the measured I_{sc} compared to the control regression line at each time by paired t-tests.

An agonist for P2Y purinergic channels, 2-thio UTP, caused significant change in the I_{sc} when applied to the apical side after 30 minutes with the lower dose of the drug (0,34 μM), compared to the control regression line ($p=0.05$). Both of the doses tested of the nonselective antagonist PPADS for P2Y receptors caused no significant change in the I_{sc} in comparison with the regression line. Washing out with the normal Krebs solution at the end of the experiment the I_{sc} seemed to decrease the I_{sc} again temporarily.

The effects of 2-thioUTP and PPADS on TER

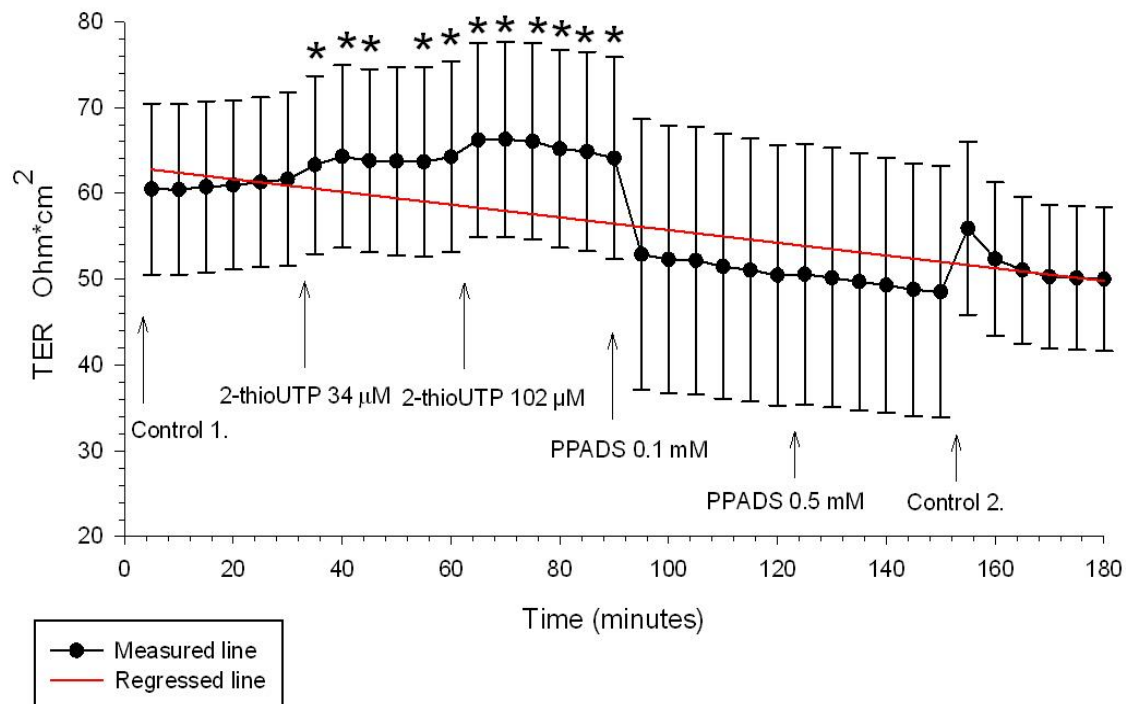


Figure 14 The effects of P2Y agonist 2-thio UTP and its antagonist PPADS on TER.

The figure shows changes in the TER when the agonist for P2Y receptors 2-thio UTP and the nonselective antagonist for P2 receptors were applied on the apical side of the RPE mouse tissue. The ordinate shows the measured value of the TER and the abscissa shows the time of the drugs in the bath solution in the Ussing chamber ($n=6$). The red line is the control regression line calculated between the last three TER measurements of each of the two control periods. The stars indicate a statistical significant difference of the measured TER compared to the control regression line at each time by paired t-tests.

The transepithelial resistance increased significantly in response to both of the 2-thioUTP doses applied to the apical bath solution for 30 minutes. The TER changed from $59,1 \pm 8,5 \text{ Ohm}\cdot\text{cm}^2$ during the last 5 minutes with Control 1 to $64 \pm 10 \text{ Ohm}\cdot\text{cm}^2$ after 30 minutes with the larger dose (102 μM) in the bath solution. The return to fresh Krebs in Control 2 did decrease the TER to $50,9 \pm 7,4$ from $59,7 \pm 11,5 \text{ Ohm}\cdot\text{cm}^2$ after 30 minutes. The effects of washing the drug away in the Control 2 measurements were not notable and it seems like the PPADS had already inhibited the effects from the P2Y agonist.

4.4 Chloride channels

4.4.1 The effect of NPPB

NPPB (4 mM) applied to the basolateral side of the RPE tissue did not cause any significant change in the short circuit current. The same dose applied at the apical side of the RPE mouse tissue however caused a highly significant decrease and reversal in the I_{sc} (see figure 19).

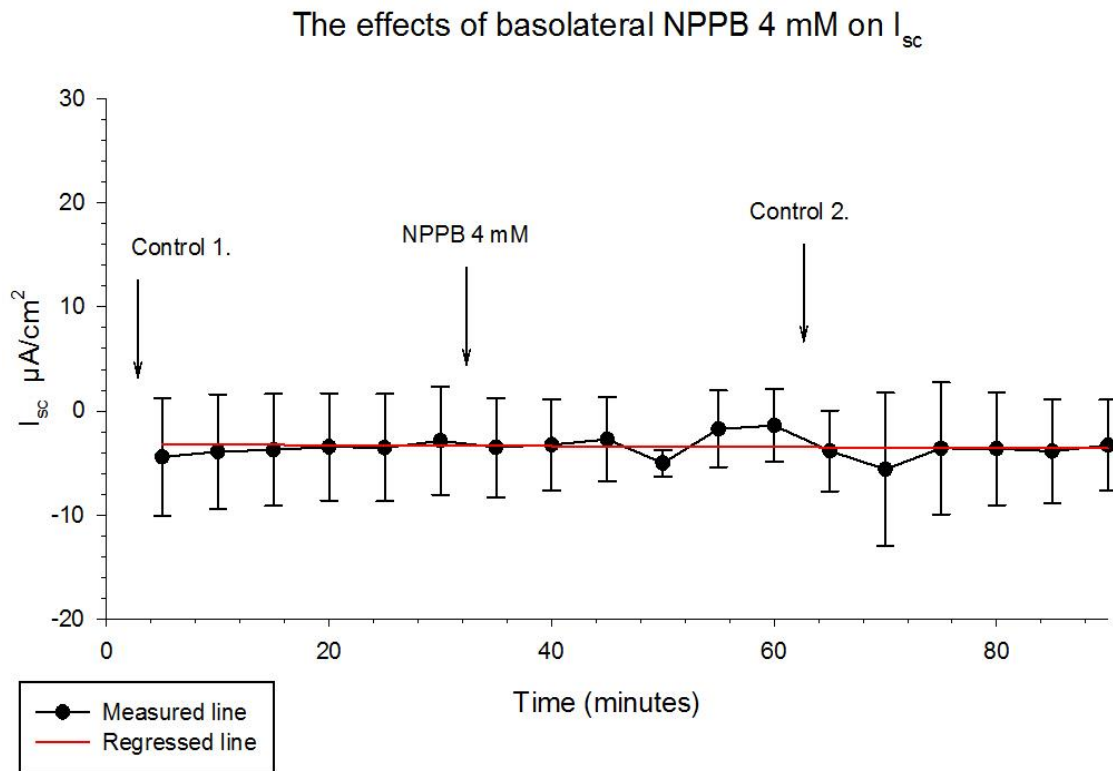


Figure 15 The effects of basolateral chloride channel blocker (4 mM) on I_{sc} .

The figure shows the change in the I_{sc} with 4 mM of the nonselective chloride channel blocker NPPB applied on the basolateral side. The blocker was applied on the basolateral side of the RPE mouse tissue. The ordinate shows the measured value of the I_{sc} and the abscissa shows the time of the drugs in the bath solution in the Ussing chamber ($n=6$). The red line is the control regression line calculated between the last three I_{sc} measurements of each of the two control periods. The stars indicate a statistical significant difference of the measured I_{sc} compared to the control regression line at each time by paired t-tests.

Applying NPPB (4 mM) to the basolateral side caused no significant change in the I_{SC} during 30 minutes of measurements. The I_{SC} was $-2.9 \pm 5.2 \mu A/cm^2$ during the last 5 minutes of the Control 1 measurements and $-1.4 \pm 3.5 \mu A/cm^2$ after 30 minutes with NPPB in the basolateral bath solution.

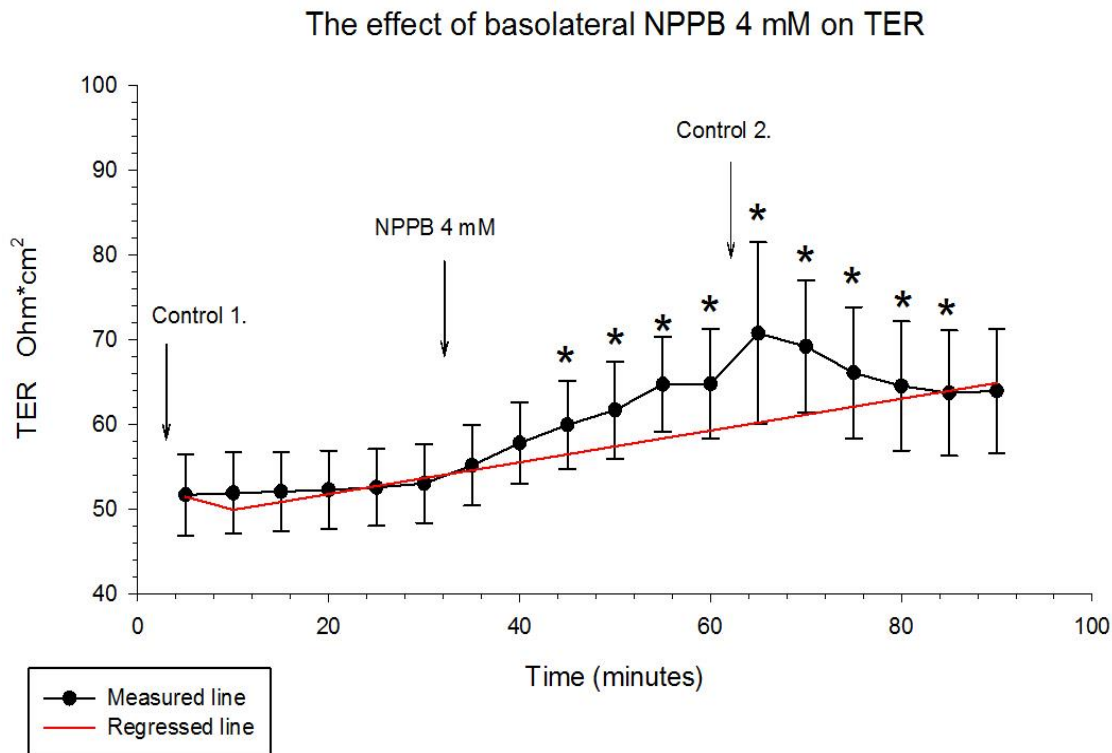


Figure 16 The effects of basolateral chloride channel blocker NPPB (4 mM) on the TER.

The figure shows the change in the transepithelial resistance changes with the nonselective chloride channel blocker NPPB (4 mM), applied on the basolateral side of the RPE mouse tissue. The ordinate shows the measured value of the TER and the abscissa shows the time of the drugs in the bath solution in the Ussing chamber (n=6). The red line is the control regression line calculated between the last three TER measurements of each of the two control periods. The stars indicate a statistical significant difference of the measured TER compared to the control regression line at each time by paired t-tests.

The TER did increase significantly with NPPB (4 mM) applied on the basolateral side of the RPE tissue, in comparison with the control regression line. The TER changed from a mean of $53 \pm 4,6$ during the last 5 minutes of the Control 1 period to $64,8 \pm 6,4 \text{ Ohm*cm}^2$ after 30 minutes with 4 mM NPPB placed in the basolateral bath solution. Control 1 measurement was really stable for 30 minutes. After the washout, the Control 2 measurements indicate that the drug was slowly and not properly washed away from the RPE tissue.

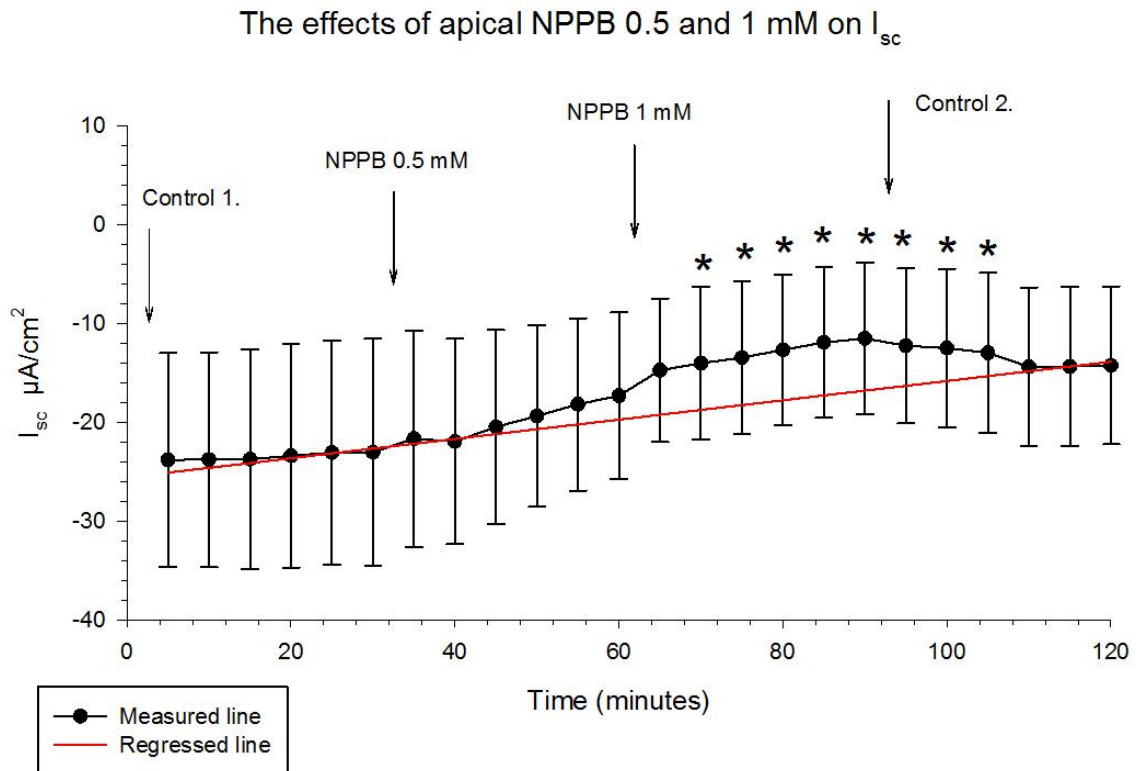


Figure 17 The effects of the apical chloride channel blocker (0,5 and 1 mM) on the on the I_{sc} .

The figure shows the change in the short circuit current caused by apical NPPB 0,5 and 1 mM applied on the apical side of the RPE tissue. The ordinate shows the measured value of the I_{sc} and the abscissa shows the time of the drugs in the bath solution in the Ussing chamber (n=6). The red line is the control regression line calculated between the last three I_{sc} measurements of each of the two control periods. The stars indicate a statistical significant difference of the measured I_{sc} compared to the control regression line at each time by paired t-tests.

Measurements with the tissue in normal Krebs solution for 30 minutes at the beginning of the experiment indicate that it was stable. When the first dose of the NPPB (0.5 mM) was added to the apical bath solution the I_{sc} decreased but not significantly. After the second apical dose (1 mM) the I_{sc} decreased significantly ($p=0.01$) after 30 minutes. The change to normal Krebs at the end of the experiment showed also a significant increase in the I_{sc} .

The effects of apical 0,5 and 1 mM NPPB on TER

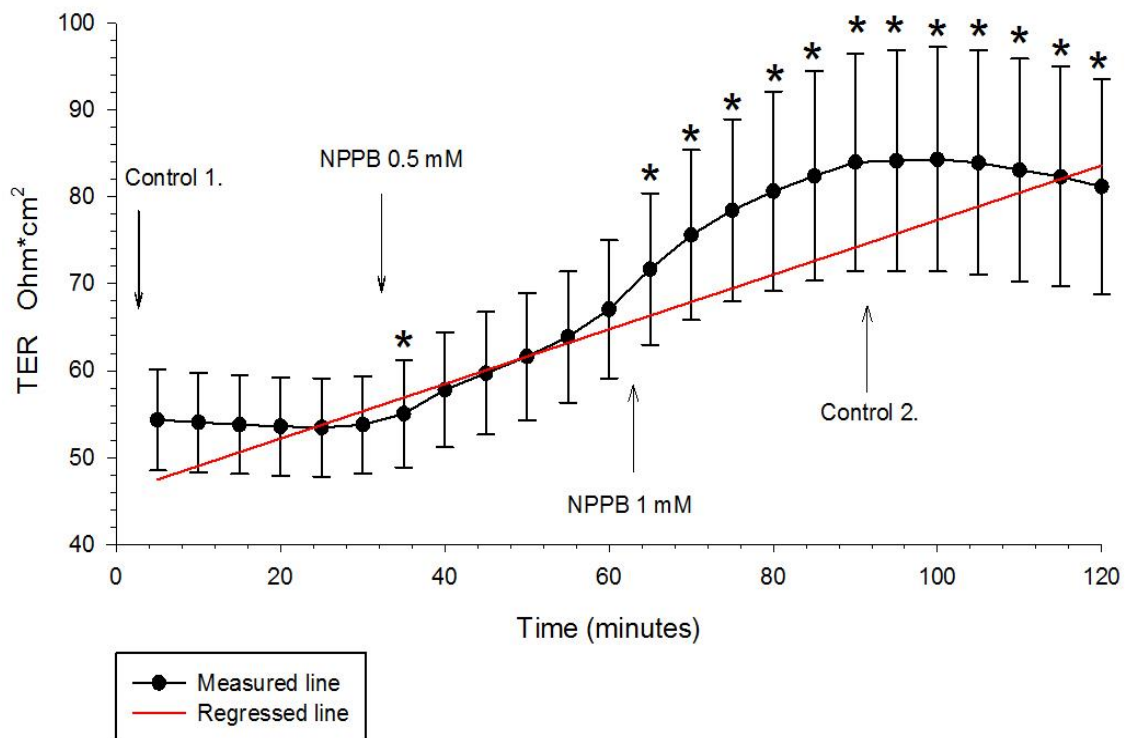


Figure 18 The effects of apical chloride channel blocker (0,5 and 1 mM) on TER.

The figure shows the change in the TER with 0,5 and 1 mM NPPB in the bath solution on the apical side of the RPE tissue. The ordinate shows the measured value of the TER and the abscissa shows the time of the drugs in the bath solution in the Ussing chamber (n=6). The red line is the control regression line calculated between the last three I_{sc} measurements of each of the two control periods. The stars indicate a statistical significant difference of the measured I_{sc} compared to the control regression line at each time by paired t-tests.

The transepithelial resistance did increase significantly with only the higher dose (1 mM) for 30 minutes as compared to the regression line ($p \leq 0.01$). The TER increased from $53,7 \pm 5,6 \text{ Ohm*cm}^2$ during the last 5 minutes of Control 1 measurements to $67 \pm 7,9 \text{ Ohm*cm}^2$ after 30 minutes with the lower dose (0.5 mM) in the bath solution, and further to $84 \pm 12,5 \text{ Ohm*cm}^2$ after 30 minutes with the higher dose (1 mM) of the antagonist. The TER did showed a very small decrease after switching to normal Krebs solution at the end of the experiment which may indicate that the drug was not being washed properly away.

The effects of apical NPPB 4 mM on I_{sc}

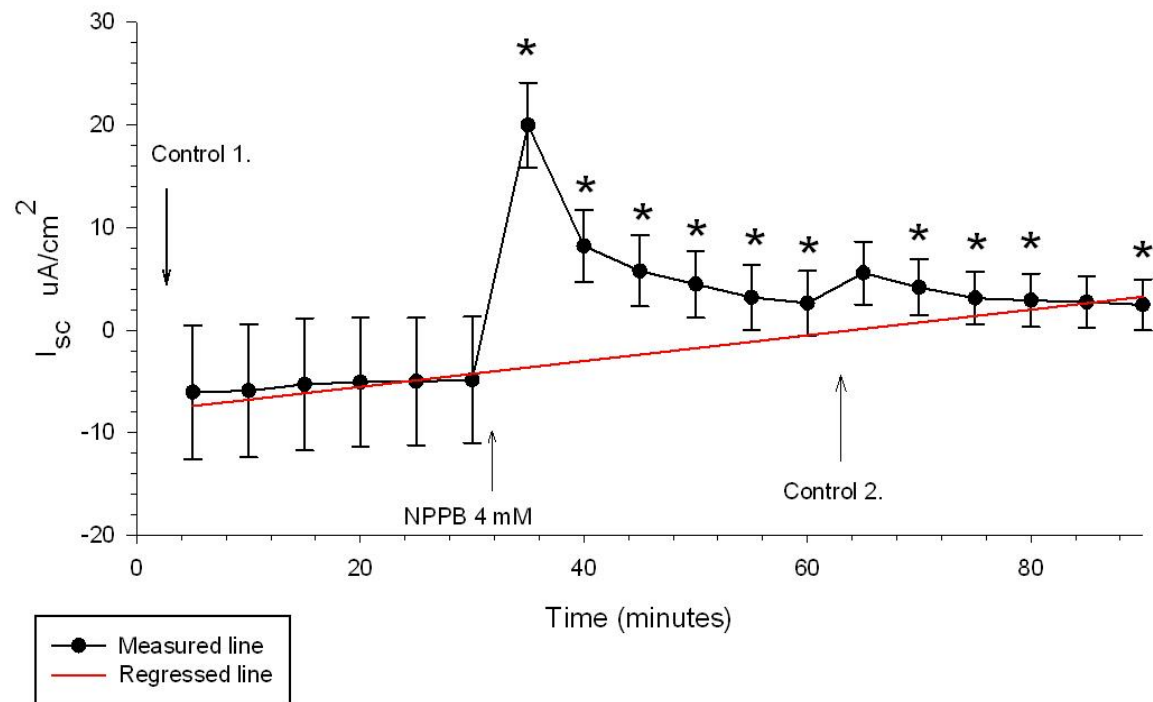


Figure 19 The effects of apical chloride channel blocker (4 mM) on the I_{sc} .

The figure shows the change in the I_{sc} with the NPPB (4 mM) in the Ussing chamber bath solution for 30 minutes. The ordinate shows the measured value of the I_{sc} and the abscissa shows the time of the drugs in the bath solution in the Ussing chamber ($n=6$). The red line is the control regression line calculated between the last three I_{sc} measurements of each of the two control periods. The stars indicate a statistical significant difference of the measured I_{sc} compared to the control regression line at each time by paired t-tests.

The short circuit current did decrease enormously when 4 mM of the nonselective chloride channel blocker NPPB was applied on the apical side of the RPE mouse tissue. The I_{sc} reversed significantly from -4.8 ± 6.5 during the last 5 minutes of Control 1 measurement to $+19.9 \pm 4.1$ after 5 minutes with 4 mM NPPB in the apical bath solution, and was stabilized at $+2.6 \pm 3.3$ after 30 minutes. The NPPB caused a significant change in the I_{sc} for 30 minutes as compared to the control regression line. It seems that the drug was not washed out with the fresh Krebs, since the I_{sc} did not decrease much during the Control 2 period.

The effects of apical NPPB 4 mM on TER

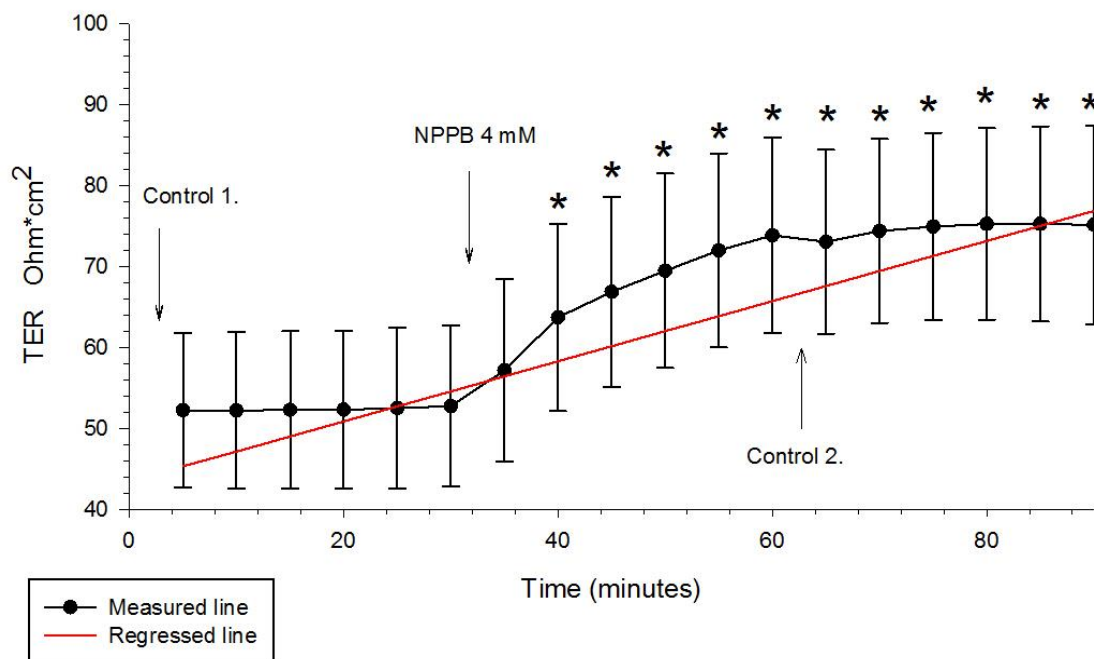


Figure 20 The effects of the apical chloride channel blocker (4 mM) on TER.

The figure shows the change in the TER when 4 mM dose of the nonselective chloride channel blocker NPPB was applied on the apical side of the RPE of a mouse tissue (n=6). The ordinate shows the measured value of the TER and the abscissa shows the time of the drugs in the bath solution in the Ussing chamber (n=6). The red line is the control regression line calculated between the last three TER measurements of each of the two control periods. The stars indicate a statistical significant difference of the measured TER compared to the control regression line at each time by paired t-tests.

The nonselective chloride channel blocker NPPB did increase the transepithelial resistance from a $52,8 \pm 9,9$ during the last 5 minutes of Control 1 measurements to $73,8 \pm 12$ Ohm*cm² after 30 minutes, with NPPB in the Ussing chamber apical bath (n=6). During the Control 2 measurement there was not much change from recordings during 4 mM NPPB and it seems that the drugs was not properly washed away with the normal Krebs at the end of the experiment.

4.4.2 The effects of CaCCinh-A01

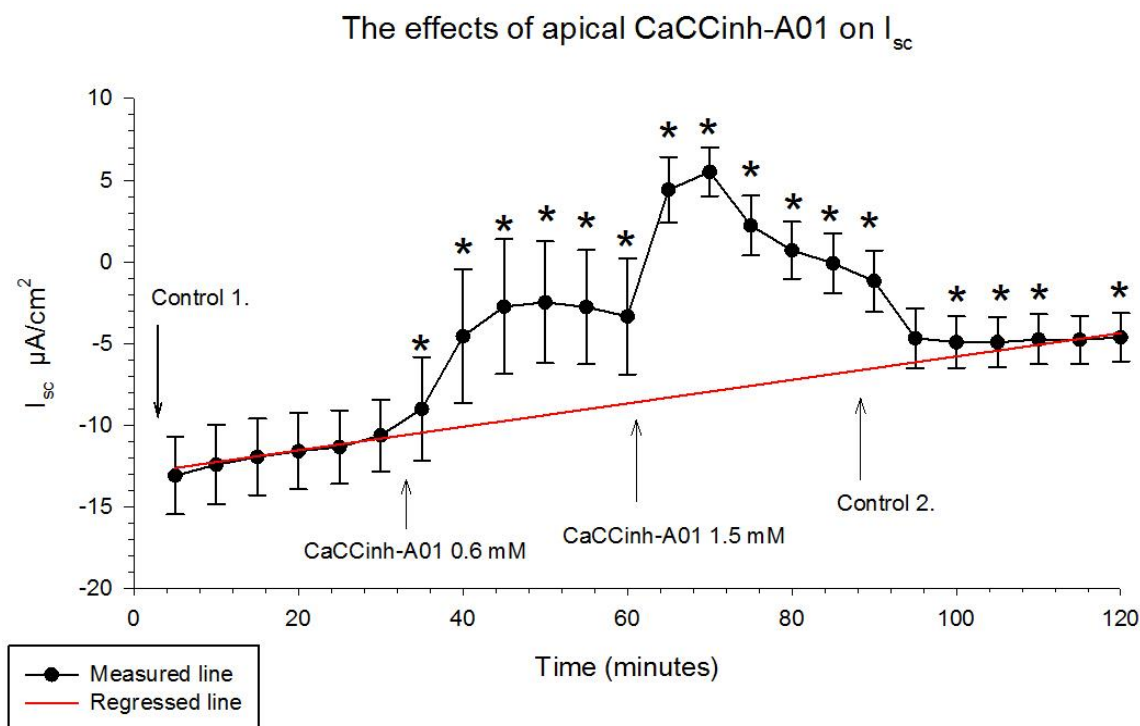


Figure 21 The effects of the apical calcium activated chloride channel agonist on the I_{sc} .

The figure shows the changes in the I_{sc} with the addition of the calcium activated chloride channel blocker CaCCinh-A01 to the apical solution only. The blocker was applied in two different doses, first 0.6 mM and then 30 minutes later 1.5 mM. During the last 30 minutes of the experiment the substances were washed away with normal Krebs solution ($n=6$). The ordinate shows the measured value of the I_{sc} and the abscissa shows the time of the drugs in the bath solution in the Ussing chamber ($n=6$). The red line is the control regression line calculated between the last three I_{sc} measurements of each of the two control periods. The stars indicate a statistical significant difference of the measured I_{sc} compared to the control regression line at each time by paired t-tests.

The chloride channel blocker CaCCinh-A01 decreased the I_{sc} significantly when applied on the apical side in response to both of the doses tested, 0.6 mM ($p=0.01$) and 1.5 mM ($p=0.03$) in comparison to the control regression line. The I_{sc} changed from $-10 \pm 2,2$ during the last five minutes of the Control 1 measurements to $-3,3 \pm 3,5 \mu A/cm^2$ after 30 minutes of the lower dose (0.6 mM) in the Ussing chamber. The higher dose (1.2 mM) reversed the I_{sc} from -3 ± 3.4 during the last five minutes of the smaller dose (0.6 mM) to $+5.5 \pm 3.9 \mu A/cm^2$ after 10 min with the larger dose (1.5 mM), similar to the apical NPPB 4 mM dose effects. After 30 minutes with the higher dose (1.5 mM) in the solution the I_{sc} was fairly stable at $-1,2 \pm 1,8 \mu A/cm^2$. After washing out the inhibitor with a fresh Krebs solution (Control 2), the I_{sc} changed from $-1,2 \pm 1,8$ during the last 5 minutes of the higher CaCCinh-A01 dose fairly sharply to $-4,9 \pm 1,6 \mu A/cm^2$ after 10 minutes of fresh Krebs solution. This indicates that the the drug was washed properly away from the RPE cells.

Effects of apical CaCCinh-A01 on TER

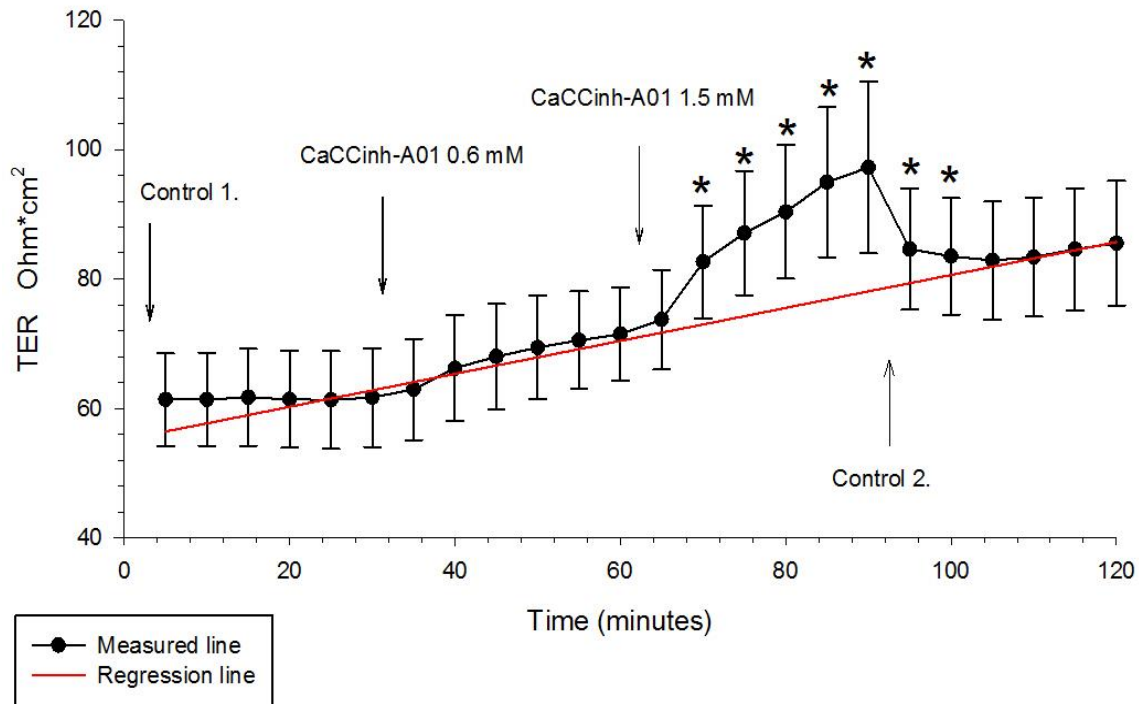


Figure 22 The effects of apical calcium activated chloride channel agonist on TER.

The figure shows how the transepithelial resistance increases with increasing level of the calcium activated chloride channel blocker CaCCinh-A01 in the apical bath solution. The blocker was applied in two different doses, first 0.6 mM and then 30 minutes later 1.5 mM dose of the blocker. The last 30 minutes of the experiment the solution was returned back to Normal Krebs (n=6). The ordinate shows the measured value of the TER and the abscissa shows the time of the drugs in the bath solution in the Ussing chamber (n=6). The red line is the control regression line calculated between the last three TER measurements of each of the two control periods. The stars indicate a statistical significant difference of the measured TER compared to the control regression line at each time by paired t-tests.

The transepithelial resistance did not increase significantly with the lower dose of the blocker. The higher dose caused a significant increase in TER after 10 minutes, which continued to increase until the 30th minute, as compared to the control regression line ($p=0.02$). The TER changed from a mean of $71,5 \pm 7,3 \text{ Ohm}\cdot\text{cm}^2$ after 30 minutes with the lower dose (0.6 mM) in the bath, and further to $97 \pm 13 \text{ Ohm}\cdot\text{cm}^2$ after 30 minutes with the higher dose. With the return back to fresh Krebs for Control 2 measurements the TER did stabilize after the increase induced by the channel blocker, and remained stabilized for 30 minutes.

4.4.3 Results from the CFTR experiments

The effects of CFTRinh-172 on I_{sc}

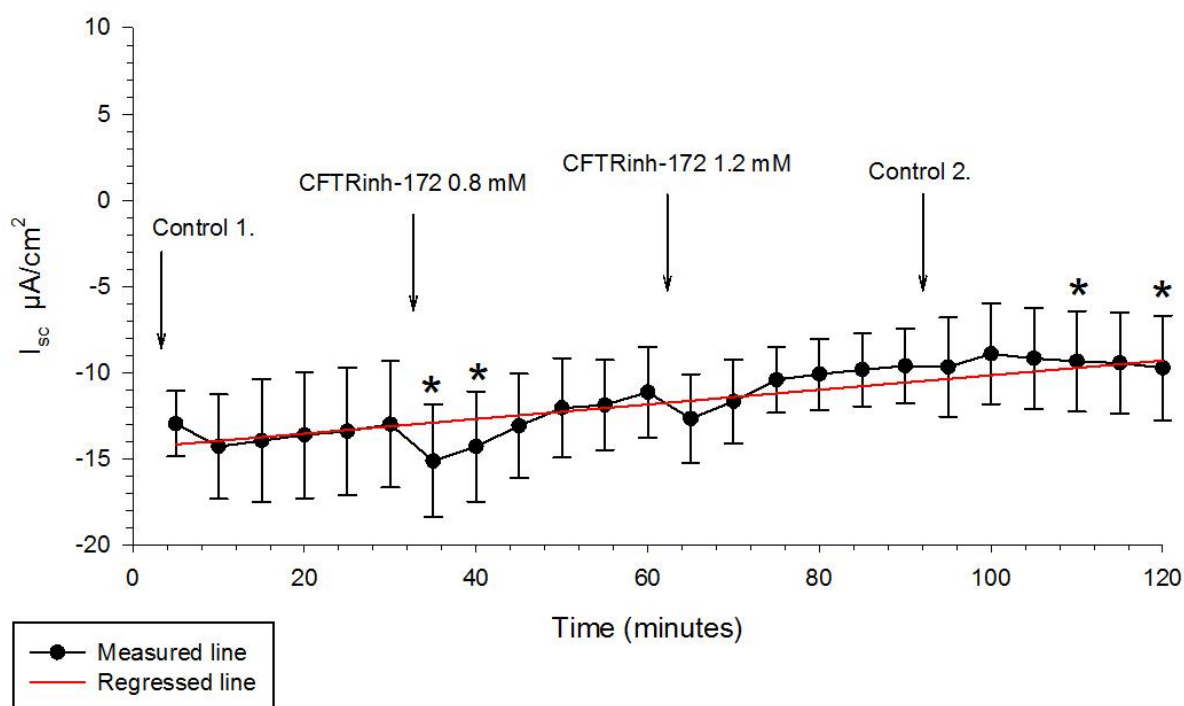


Figure 23 The effects of apical CFTR chloride channels blocker on the I_{sc} .

The figure shows how the I_{sc} changes with the CFTR chloride channel blocker CFTRinh-172 in the bath solution for one hour. The blocker was applied in two different doses, 0,8 and 1,2 Mm. The ordinate shows the measured value of the I_{sc} and the abscissa shows the time of the drugs in the bath solution in the Ussing chamber ($n=6$). The red line is the control regression line calculated between the last three I_{sc} measurements of each of the two control periods. The stars indicate a statistical significant difference of the measured I_{sc} compared to the control regression line at each time by paired t-tests.

The CFTR chloride channel blocker CFTRinh-172 did increase the I_{sc} significantly during the first 10 minutes in the bath solution with the lower dose of the antagonist (0.8 mM) compared to the regression line ($p=0.03$). The I_{sc} changed from $-13 \pm 3,7$ during the last 5 minutes of the Control 1 measurement to $-14,1 \pm 3.2 \mu A/cm^2$ after the first 10 minutes with the 0.8 mM dose of the antagonist in the Ussing chamber. After that the I_{sc} decreased gradually for the next 60 minutes with both the lower dose and the higher dose (1.2 mM) to $-9.6 \pm 2.1 \mu A/cm^2$. The changes were not significant as compared to the control regression line ($p=0.22$).

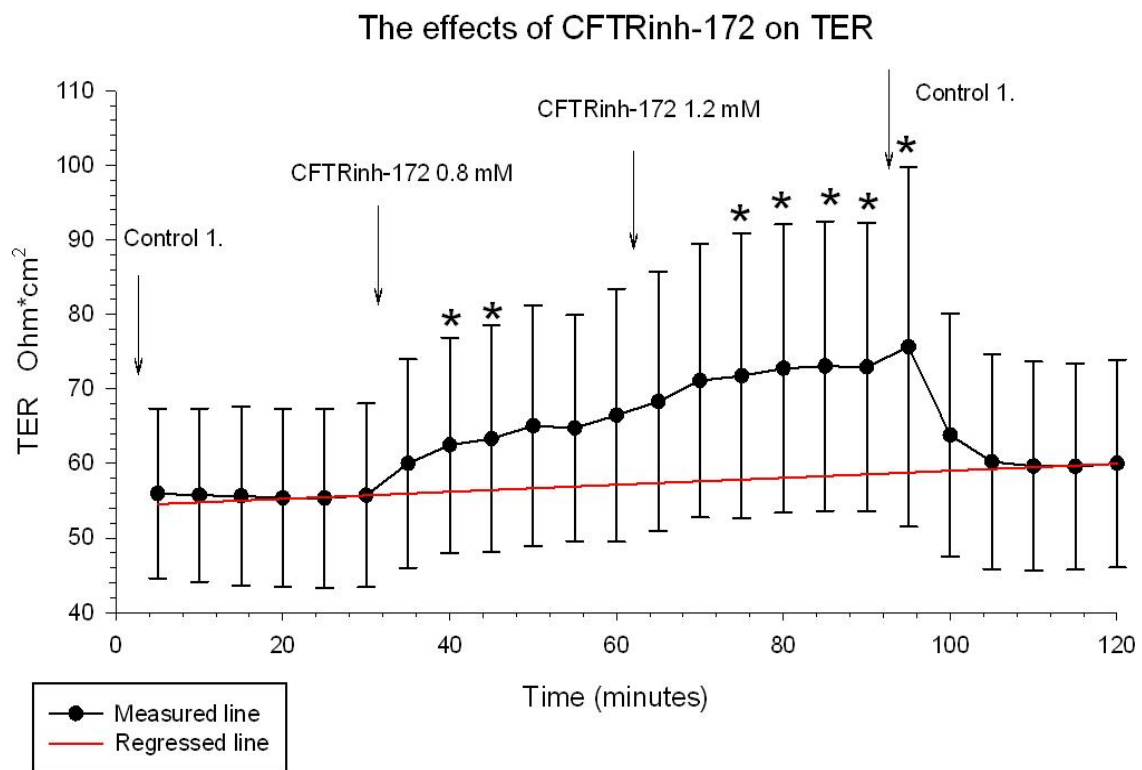


Figure 24 The effects of apical CFTR chloride channel blocker on TER.

The figure shows how the transepithelial resistance changes with the CFTR chloride channel antagonist CFTRinh-172 for 60 minutes in the Ussing chamber bath solution. The ordinate shows the measured value of the TER and the abscissa shows the time of the drugs in the bath solution in the Ussing chamber (n=6). The red line is the control regression line calculated between the last three TER measurements of each of the two control periods. The stars indicate a statistical significant difference of the measured TER compared to the control regression line at each time by paired t-tests.

Control 1 measurements were stable for 30 minutes and did not show much variation from the estimated control regression line. The first ten minutes with the lower dose of the blocker (0.8 mM) caused a significant change in the TER compared to the regression line ($P=0.02$). TER increased steadily for 60 minutes from 56 ± 12 during the last 5 minutes with the Control 1 measurements to 73 ± 19.3 Ohm*cm² after 30 minutes of the higher dose of the blocker (1.2 mM). The TER decreased fairly sharply with normal Krebs in the end of the experiment, from 73 ± 19.3 Ohm*cm² during the last 5 minutes with the higher dose of the blocker (1.2 mM) to 60 ± 14 Ohm*cm² after 30 minutes of Control 2. So it seems like the drug was washed properly away from the RPE cells and was not affecting them any further.

4.5 Results from genotyping mice DNA for $Crb1^{rd8}$

During the dissection of the eye tissue for the Ussing experiments we noticed that some of the eyes had lighter areas on the retina/RPE layer of the eye. The lighter areas seemed to be yellowish in color and large enough to worry about possible retinal degeneration of some sort, for example comparable to retinitis pigmentosa (RP) described earlier in the introduction chapter. The reason we wanted to sort, for example if the mice had retinitis pigmentosa is the fact that in early RP disease the patients have similar yellow areas to the ones we observed. We therefore decided to examine this further by genotyping for $Crb1^{rd8}$ that is a known mutation found in some C57BL6/J mice showing retinal degeneration, to exclude the possibility that I was working with eyes that have this degeneration. (Mattapallil et al. 2012).

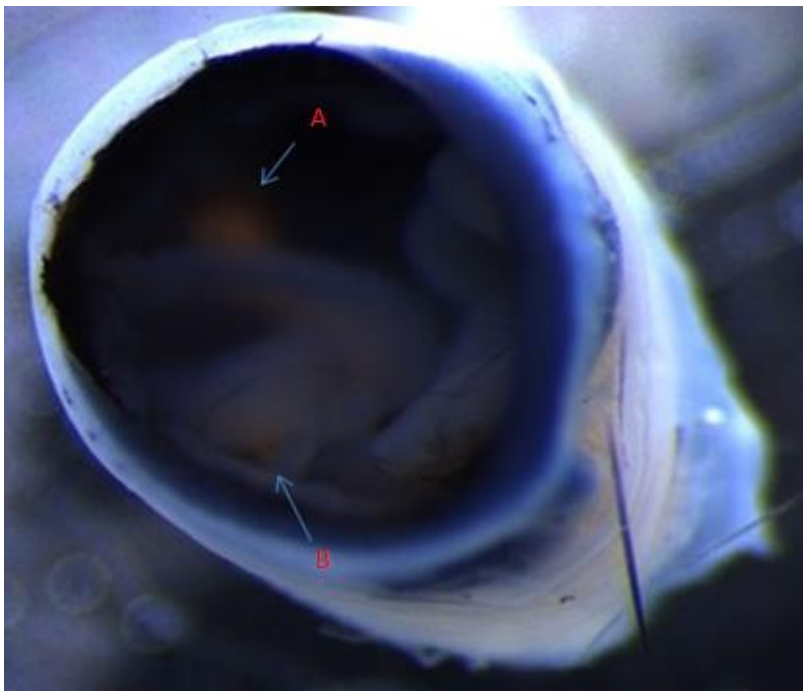


Figure 25 Spots seen in the mouse (C57BL6/J) eye tissue.

The cornea and the lens have been removed from the eye and the retina is on the top of the inner eye and the sclera is covering the outer eye. A and B: yellow areas that are possibly drusen are seen through the retina and the RPE tissue.

We attempted to analyze 3 of our stock mice (C57BL6/J) for the $Crb1^{rd8}$ mutation. I was only able to amplify efficiently from one of the DNA samples. It did not indicate that the mouse had the $Crb1^{rd8}$ mutation that causes the eye disease Retinitis Pigmetosa (Figure 26).

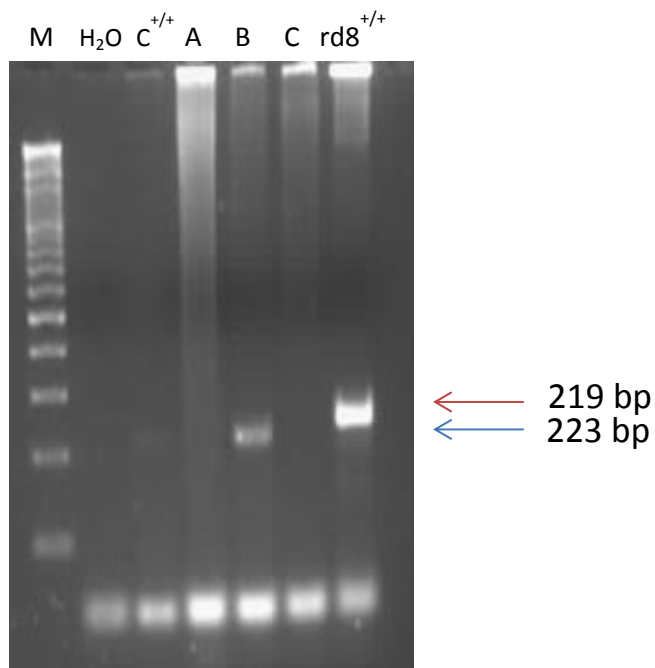


Figure 26 Agarose gel electrophoresis on amplicons from mutation analysis of the $Crb1^{rd8}$ mutation.

Genotyping of the $Crb1^{rd8}$ mutation on DNA from C57BL6/J. Columns from the left: M) The size marker, H₂O) Control sample without DNA, C^{+/+}) Control mouse DNA. A-C) DNA from mice used in the experiments. rd8^{+/+}) DNA with the $Crb1^{rd8}$ mutation. The DNA from the rd8 mutation has 248 base pairs and the DNA from our mice was 219, wild type is 223 base pairs, indicating that the DNA from our mice does not have the rd8 mutation.

5 Discussion

5.1 Ussing Experiments on mouse RPE tissue

The work described here shows that the mouse RPE can be tested in Ussing chamber experiments to measure both the ionic current of the tissue and the transepithelial resistance (see figures 5-24). This is the first time that native mouse RPE tissue has been maintained alive for up to 4-5 hours in Ussing chambers. There is one other previously published experiment on maintaining RPE mouse tissue alive in Ussing chambers but it stayed alive only for a few minutes (Bosl et al. 2001). Experiments have been performed previously measuring the net short circuit current in bovine, frog, canine and rat RPE tissue (Strauss, 2005). Results from our experiments showed that both purinergic receptors and chloride channels can affect the short circuit current and the transepithelial resistance of the mouse RPE tissue (see figures 5-24).

Activation of the purinergic receptors decreased the I_{SC} with most of the substances tested, such as with activation of P2YR and P2X₇R receptors on the apical side (see figures 5,11,13) or they caused no significant change in the I_{SC} for example with the activation with different drugs of P2XR (see figure 9) and activation on P2 receptors on the basolateral side (see figure 7). The TER was increased with activation with different drugs of P2R, for an example P2YR, β y-meATP (see figure 10) and the specific antagonist for P2X₇ receptors, A 839977 (see figure 12).

The results from the experiments performed to study the role of chloride channels in ionic transport across the mouse RPE were unexpected since they showed greater effects on the apical side compared to the basolateral side of the RPE mouse tissue (see figures 15-20), which is the opposite to what we had expected based on published experiments in other species with chloride channels on the RPE tissue (Wimmers et al., 2007). Blocking the calcium activated chloride channels on the apical side caused a significant change in the I_{SC} and the TER that confirms the CaCCsR are situated on the apical side of the mouse RPE tissue (see figures 21, 22). Blocking the CFTR channels did however not cause great change in the I_{SC} but did affect the TER more (see figures 23, 24).

The results will now be discussed in detail for the purinergic receptors and chloride channels separately.

5.2 The role of purinergic receptors in transepithelial ion transport and resistance

The purinergic receptor agonist ATP significantly decreased ionic current when added to the apical side of the RPE tissue (see figure 5). There are two possible explanations for this decrease in the I_{SC} , either there were fewer anions (Cl^- for example) that were being transported from the apical side over to the basolateral side or there were more cations (Ca^{2+} or K^+ for example) in comparison to anions transported from the apical side to the basolateral side. The I_{SC} did not decrease as much during the basolateral ATP experiments (see figure 7), as compared to the apical experiments, but the I_{SC} nevertheless did decrease significantly with the higher dose (3 mM) of the agonist. Earlier research have indicated that purinergic receptors are found on both the apical and the basolateral sides of the

RPE in rats, but our results indicate that the purinergic receptors have more effects on the I_{SC} on the apical side of the mouse RPE tissue (Mitchell and Reigada 2008) .

The TER did not show any significant change neither with the apical ATP nor with the basolateral ATP which may be surprising since the I_{SC} changed significantly with the substance on each side (see figure 6,8). The reason could be because the measurement of TER involves measuring the resistance of the entire tissue, and what creates this resistance is one or both of the following: how tight the junctions are between the RPE cells and how many ion channels are open on the cells. The tighter the junctions are between the RPE cells the higher resistance is measured in the tissue, and the more ion channels that are closed each time the higher resistance is measured in the RPE tissue.

The ATP has been shown to induce ionic current in rat the RPE cells with the patch clamp recording technique (Ryan et al. 1999), and also to increase transepithelial chloride ion and fluid transport (Collison et al. 2005).

The experiments on the apical and the basolateral P2 receptors with ATP did not provide a clear answer as to which receptors subtypes of the ATP receptors were affecting the ion transport and the transepithelial resistance of the RPE tissue. For that reason we did further experiments with specific P2 receptors agonist and antagonist for P2XR, P2YR and on P2X₇R.

The treatment with both the P2X purinergic receptor agonist $\beta\gamma$ -meATP and its antagonist PPADS caused almost no change in the short circuit current over two hours period (see figure 9). On the other hand, the TER changed significantly for the whole time with both $\beta\gamma$ -meATP and PPADS in the bath solution for 30 minutes each substance (see figure 10). The TER started increasing significantly when the nonspecific P2X ion channels were activated with $\beta\gamma$ -meATP for 30 minutes (see figure 10). The TER did however not change much with the addition of the antagonist for the same receptors for the next 30 minutes, which leaves us with a question: It is clear from the results that the $\beta\gamma$ -meATP did increase the TER but it is unclear why PPADS did not reduce that affect. There can be two reasons for that, either the dose of the antagonist was not high enough to reduce the effects from the agonist or it could be that the antagonist cannot push the agonist away from the receptors due to lack of specificity. It is more likely that the agonist was the only one causing an increase in the TER since the TER did not change at all when the antagonist was added to the bath solution. From these facts we estimate that the P2X agonist $\beta\gamma$ -meATP and its antagonist PPADS do not affect the ion current in mouse RPE and only P2X agonist $\beta\gamma$ -meATP had a significant affect the TER of the mouse RPE tissue. These results are consistent with studies performed by Ryan et al. (1999) where the cation current induced by ATP was found to be insensitive to PPADS. Until this date there is no research that we are familiar with that shows that PPADS and $\beta\gamma$ -meATP can induce change in the transepithelial resistance of the RPE tissue.

It seems that the P2X₇ receptor does affect the I_{SC} of the mouse RPE tissue but the significant changes were transient with the lower dose of its agonist (see figure 11), and the higher dose of the

agonist (BzATP) did not cause any significant change in the I_{SC} (see figure 11). The antagonist for the $P2X_7$ receptor, A 839977, however caused the I_{SC} to increase significantly for 25 minutes so it may be that either the $P2X_7$ was affecting the tissue the whole time, but just not significantly, or the antagonist did have an independent effect on the I_{SC} of the mouse RPE (see figure 11). Both of the drugs were washed properly away with the normal Krebs solution in the end of the experiment that caused the I_{SC} to decrease again (see figure 11).

Activating the $P2X_7$ receptors with BzATP did cause a significant increase in the TER after 25 minutes of the higher dose of the agonist in the Ussing chamber. The TER however continued to be statistically significantly different compared to the estimated regression line with both doses of the $P2X_7$ blocker (see figure 12). The fact that TER had already started to increase significantly with the higher dose of the $P2X_7$ agonist makes one wonder if the effects were from the antagonist, or due to increasing effects from the agonist. It seems that the higher dose of the A 839977 antagonist can block the $P2X_7$ receptors on the apical side and affect both the short circuit current and the transepithelial resistance of the mouse RPE tissue. The normal Krebs solution in the end of the experiment did wash away the effect from the $P2X_7$ agonist as the transepithelial resistance decreased again promptly and significantly (see figure 12).

BzATP has been shown to induce calcium influx and apoptosis of RPE cells by activating the $P2X_7$ receptor in studies with cultured human eye tissue (Yang et al. 2011). The calcium influx may then induce transepithelial transport over the RPE tissue by activating calcium activated chloride channels on the basolateral side of the RPE tissue (Peterson et al. 1997). A 839977 has been shown to block BzATP induced Ca^{2+} influx in human, rat and mouse in 1321N1 glial cell line expressing $P2X_7$ receptor (Jiang, 2012).

The $P2Y$ agonist 2-thioUTP did not cause much effect on the I_{SC} of the mouse RPE tissue, and only transient significant effects with the lower dose of the agonist (0.1 mM) were found (see figure 13). It seems that either the dose was not high enough or that the $P2Y$ receptors are not having any effect on the net ion transport of the mouse RPE. Human RPE cells express $P2Y_{1,2,4,6}$ (Tovell & Sanderson, 2008). But upto this point it is not known which subtypes of the $P2Y$ receptors are expressed in the mouse RPE. An extensive literature search suggests that this has not been examined in the mouse RPE. The TER did increase significantly with both doses of the agonist for 60 minutes (see figure 14). Addition of the antagonist for $P2Y$ receptors PPADS caused the TER to decrease again, which shows that the PPADS functions as an antagonist to the stimulating effects mediated the $P2Y$ receptors on the TER of the mouse RPE tissue (see figure 14). It conclusion is that the $P2Y$ receptors affect the TER of the mouse RPE tissue and not the net ion transport. The change back to normal Krebs in the end did not seem to evoke any change in the TER for 30 minutes since the antagonist of the $P2Y$ receptors (PPADS) had already blocked the effects from the $P2Y$ receptors stimulated by 2-thioUTP.

5.3 The role of chloride channels in transepithelial ion transport and resistance

The chloride channels are thought to have an important role in the transepithelial transport of water by the RPE tissue (Reichhart and Strauss 2014) (see figure 27). The ion transport of the RPE tissue should therefore theoretically be driven by the transport of the chloride channels and the same channels should control a big part of the I_{SC} of the RPE tissue. For that reason experiments were performed with blocking chloride channel blockers on the RPE tissue: to measure any change in the net ion current, i.e. I_{SC} , of the RPE with the chloride channels blocked. According to Strauss (2005), the Na/K-ATPase provides a gradient for the Na/K/2Cl cotransporter to transport Na^+ ions into the RPE cells and with them also the K^+ and Cl^- ions. The chloride ions are then transported over to the choroid by chloride channels situated on the basolateral side of the mouse RPE tissue (such as calcium activated chloride channels, CFTR chloride channels, or ClC chloride channels) (see figure 2). The results of our experiments do not fully agree with these previous studies and will be discussed further here below:

The effects of the nonspecific chloride channel blocker (NPPB) were far greater on the apical side compared to the basolateral side, as in the series of experiments with the highest dose (4 mM), the blocker caused no significant change on the basolateral side but a huge $25 \mu\text{Amps}/\text{cm}^2$ change on the apical side, although the effects on the apical side decreased quickly (see figures 15-20). The TER did also increase significantly in response to the nonspecific chloride channel blocker on both apical and the basolateral side and the effects were seemingly not washed away with the normal Krebs solution at the end of the experiment, which indicates that most likely the drug was not washed away properly. With apical NPPB it is also quite likely that the higher dose of the chloride channel blocker may have damaged or even killed the RPE tissue, since the I_{SC} never recovered after it decreased to close to zero I_{SC} after the drug was applied to the bath solution. The NPPB chloride channel blocker is a general chloride channel blocker, and the fact this blocker is not specific makes it difficult to estimate which type of chloride channels it was affecting. However it is clear from the present results that chloride channels have in general an important role in mediating the short circuit current of the mouse RPE as seen in other mammals (Schultz et al. 1999).

The series of experiments with the lower doses of the NPPB blocker (0,5 and 1 mM) the lower dose did not cause a significant change in the I_{SC} or the TER when applied on the apical side (figures 20,21). The larger 1 mM dose however did decrease the I_{SC} and increased the TER significantly; the effects of the blocker were washed partly with the normal Krebs solution in the end of the experiment. Both the 1 mM dose and 4 mM dose of the nonspecific chloride channel blocker did cause greater effects on the TER as compared to the short circuit current (see figure 16,18,20). Until now the chloride channels have been thought to be important in transporting water and ions from the RPE on the basolateral side, and over to the choroid but not from the apical side of the RPE cells (see Figure 2) (Wimmers et al., 2007).

The fact that the specific calcium activated chloride channel blocker CaCCinh-A01 decreased the short circuit current of the RPE cells confirms the important role of the calcium activated chloride channels in transporting chloride ions across the RPE cells (see figure 21). The unexpected results in this case were how large a decrease the blocker caused on the apical side of the RPE cells (see figures 21, 22). Until now the channels have been suggested to be situated on the basolateral side of the RPE cells (Wimmers et al., 2007). Both of the doses of the blocker that were tested caused a significant decrease in the I_{SC} , which was reversed completely with wash-out by normal Krebs at the end of the experiments. The higher dose of the calcium activated chloride channel agonist did increase the TER significantly but not the lower dose. The effects on TER caused by the antagonist were also washed away with normal Krebs at the end of the experiment (see figure 22).

The CFTR channels do not seem to play a great role in mediating the ionic current across the mouse RPE tissue. The blocker CFTRinh-172 did increase the I_{SC} significantly for the first 5 minutes when the lower dose of the blocker was applied to the bath solution, which is surprising since the CFTR channels are thought to transport chloride ions across the RPE tissue, and we therefore expected to see a decrease in the I_{SC} with the blocker in the bath solution (see figure 23) (Wimmers et al., 2007). The increase of the I_{SC} was transient but the blocker caused a persistently significant change in the TER with both of the doses of the blocker tested. It seems that the CFTR channels are present on the apical side of the mouse RPE tissue (see figure 24). The smaller dose did increase the TER gradually for 30 minutes and the larger dose did cause significant change in the TER during the last 20 minutes it remained in the bath solution (see figure 24). Thus, our results indicate that the CFTR have an effect on the TER of the mouse RPE tissue but do not affect the net ion transport to a great extent. The CFTR are not just chloride channels but as the name says they are thought to be transmembrane regulator, and are supposed to regulate other channels, for example Na^+ channels on the bronchial epithelium (Greger 2000).

These results indicate that the chloride channels that have been thought to be situated only on the basolateral side of the mouse RPE tissue are also located on the apical side of the RPE tissue based. This suggests that perhaps the original theory of the chloride ion transport over the basolateral membrane to the choroid side needs revision (Strauss, 2005). Our results indicate that the main driving force of water over the RPE is with driving forces from chloride transport by showing how much the chloride channels affect the short circuit current. However the results indicate that the theory of which side the main chloride channels are situated is less reliable.

Both NPPB and CaCCinh-A01 caused similar effects on the apical side of the mouse RPE tissue and the ion current decreased more when the substances were added to the apical side than to the basolateral side. From this data it seems that the chloride ion current in the mouse RPE tissue (see Figure 2) is not carried in the same way as the chloride ion current across the RPE of other animals. It is clear that the present results are in contrast with earlier studies and lead to an idea of a new model of the chloride transport through RPE cells (see Figure 27).

The main questions that arise from the results include: Are there more chloride channels situated on the apical than the basolateral side on the mouse RPE tissue? And what channels are the most important in transporting chloride ions from the intracellular space of the RPE cells across the basolateral side to the choroid side? Chloride channels have been discovered on the basolateral side of the RPE tissue, for an example the calcium dependent chloride channels and CFTR in the canine RPE (Loewen et al., 2003) and CIC-2 channels in human RPE (Wimmers et al. 2007). Could it be that the mouse RPE tissue is different than other RPE animal tissues with respect to chloride channels and ion current? Or could it be that with respect to other RPE mammals the number of chloride channels on the apical side has been underestimated? Could it be that Ussing chambers experiments do not give good results of the ionic current in the mouse PRE tissue? Other techniques besides Ussing in recording ionic currents across cell membranes is the patch clamp technique, that measures both single ion channels and all ion channels on one single cell (Reichhart & Strauss, 2014). There are also techniques to measure the concentration of intracellular calcium with Ca^{2+} imaging, which makes it possible to estimate the function of second messenger systems of the RPE cells, and estimate the activation of ion channels activated, by intracellular calcium (Reichhart & Strauss, 2014). Ussing experiments are unique for the purpose of studying both the apical to basolateral function in transepithelial transport of ions by measuring the I_{SC} and to estimate the whole short circuit current as well as the resistance across the tissue with the time factor included.

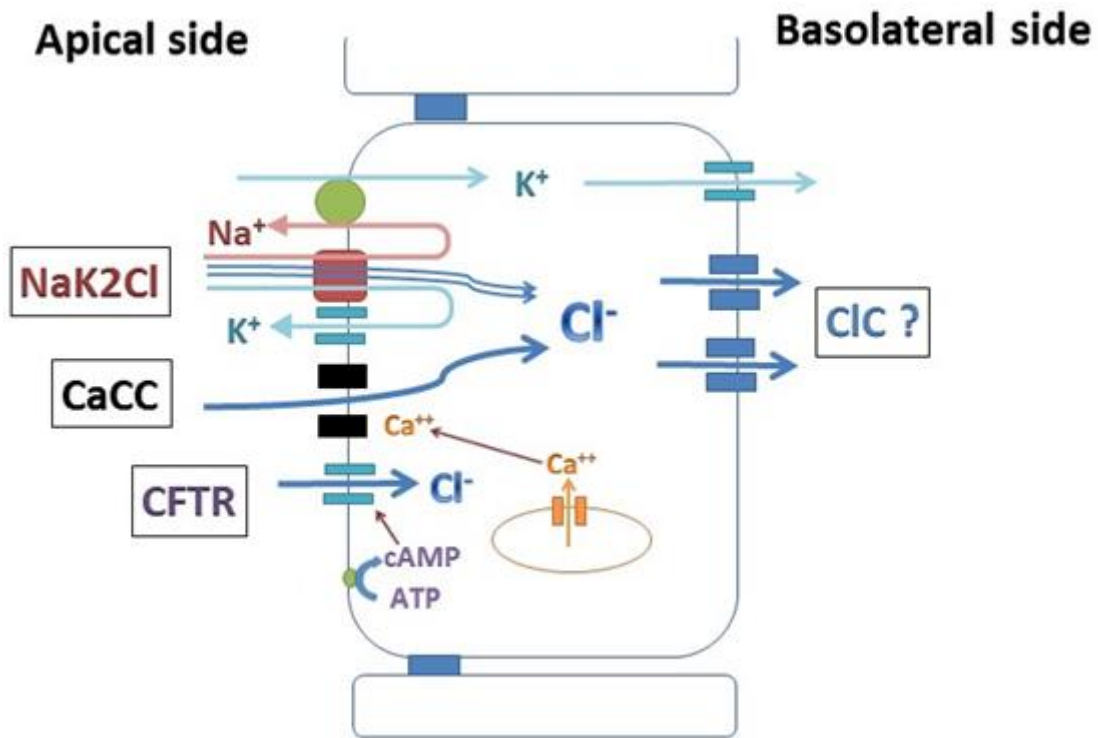


Figure 27 Model of ion transport mechanism based on our results.

The figure shows the model of ion transport mechanisms of the RPE tissue (see figure 15-24) with modifications based on our experimental results. On the apical side there is a gradient for Na⁺ into the cell provided by the activity of the apical Na/K-ATPase. The gradient is used to transport Cl⁻ into the cell via activity of the Na/K/2Cl cotransporter. Chloride diffuses also through different chloride channels like CaCC (calcium activated chloride channel) and CFTR (cystic fibroses transmembrane regulator). Cl⁻ leaves the cell on the basolateral side possibly through ClC chloride channels. cAMP: cyclic adenosine monophosphate.

5.4 Limitations of the data

Culturing of RPE tissue cells was not successful, and separating the RPE from the retina, choroid and sclera were not accomplished without destroying the RPE. The RPE cells form a thin and vulnerable layer that made the isolation of the tissue very difficult. The main drawback of the present research is the fact that the RPE preparation in the Ussing chambers was not independent but attached to the retina, choroid and sclera. This fact should not affect the results of the measurements since the photoreceptors of the retina are an unlikely source to affect the short circuit current since the photoreceptors are not as polarized as the RPE cells (Wimmers et al., 2007). The sclera and choroid are also very unlikely to affect the short circuit current measurement of the RPE, the sclera is a fibrous tissue that doesn't have much of ion channels involved in transport and the choroid is made of endothelial cells and the ion transport of the endothelial cells in the choroid does not have one direction like the RPE cells, as measurements in the Ussing chambers (see chapter 3.2).

Another part that might interfere with the results from the measurements of the RPE preparation are the Müller cells found in the retina, which are one type of retinal glial cells. Their role among other functions is to maintain the retinal extracellular environment by regulating K⁺ in the subretinal space

and possibly directing water flux from the interstitial fluid of the photoreceptors and the subretinal space to the vitreous to protect the photoreceptors from inappropriate (Hamann et al. 1998; Strauss 2005; Wimmers et al. 2007). This activity could possibly affect the results of the measured I_{SC} in the RPE. The fact that the control tissues were in some experiments unstable is also a drawback but we calculated both of the control periods at the beginning of each experiment and at the end to counteract this. We also did a whole series of experiments with only Krebs present in the baths for 2.5 hours that showed stable measurements (see Figure 4).

There is no certainty that the drugs didn't diffuse over to the other side of the RPE cell tissue and affected the transport through the receptors or channels situated there, but from our results seems that the drugs do not diffuse across to the other sides, since for example the NPPB experiments with the 4 mM dose showed that the drug only affected the I_{SC} and TER when applied to the apical side but when applied to basolateral side the antagonist did not cause effect on short circuit current, only the TER (figure 16,18 and 20), which indicates that the drugs only affected the side it was applied to. The sclera is made from collagen tissue and can possible function as a diffusion barrier, which might therefore affect the measurements of the short circuit current by inhibiting the diffusion of the drugs from the basolateral side to the RPE tissue (Wen et al. 2013). However both basolateral ATP and NPPB showed effects that indicate that the sclera did not block their diffusion.

5.5 Next steps

It is important to find out more about how ion currents flowing through RPE cells behave in healthy animal models, and from there find out what happens in the tissue that may cause RPE and retinal diseases and what are the consequences of such changes.

The next researches should include more experiments on the mouse RPE tissue without the sclera in the Ussing chamber preparation, to see if the sclera is effecting the measurement of the ion current. It would be good to repeat the experiments with the drugs on the basolateral side, such as ATP, NPPB and CaCCinh-A01 without the sclera and see if that gives different results.

The next steps with the purinergic receptors could be to confirm the presence and location of the P2Y receptors on the mouse retinal pigment epithelium. It is of further interest to examine the net ion current across the mouse PRE in purinergic receptor knockout mice, and see how it affects the ion transport.

Further experiments should include research on other types of chloride channels, such as CIC channels that may be situated on the apical and the basolateral side of the mouse RPE tissue, since they have been thought to be one of the most important channels for demonstrating the ion current of RPE tissue.

Such research work could involve both patch clamp measures where one chloride channel can be examined at a time, for example the calcium activated chloride channels, the CFTR chloride channels and also more research on which side most of the chloride channels are localized. There are many mouse models available to further examine the role of chloride channels in mouse models with RPE dysfunction and retinal diseases like AMD, Stargardt, Retinitis Pigmentosa and other similar. There is a good reason to study the ion currents of the RPE in animals, particularly with respect to the previously mentioned eye diseases, since most of them show abnormal ionic transport in the retinal pigment epithelium of the eye.

6 Conclusion

The purinergic receptors and the chloride channels affect the short circuit current and the transepithelial resistance of the mouse RPE cells. The experiments with the purinergic receptors showed that purinergic receptors are situated on both sides of the mouse RPE tissue, and influence the I_{SC} of the RPE by decreasing it, although to a small extent. There was more effect from the purinergic receptors found on the apical side however, and it seems there are more purinergic receptors found on the apical side of the mouse RPE tissue. There seems to be both P2Y and P2X receptors expressed on the mouse RPE tissue and both of them affected the resistance of the tissue.

The experiments showed that there were more effects of the chloride channel and the calcium activated chloride channels found on the apical side compared to the basolateral side of the mouse RPE tissue. There were great effects found with both nonspecific chloride channels activated and calcium activated chloride channels and the I_{SC} of the mouse RPE and its resistance. It is clear that the calcium activated chloride channels on the apical side of the RPE tissue have great influence on the whole ionic current across the RPE mouse tissue. The CFTR chloride channels do not seem to influence much the I_{SC} of the mouse RPE tissue but it affected the tissues resistance.

There is need for further experiments on the chloride channels of the RPE tissues and that should include research on both healthy mouse models and comparison with mice that have different retinal diseases, such as AMD.

References

- Ambati J, Fowler BJ (2012) Mechanisms of age-related macular degeneration. *Neuron* 75(1):26-39 doi:10.1016/j.neuron.2012.06.018
- Arden GB, Constable PA (2006) The electro-oculogram. *Progress in retinal and eye research* 25(2):207-48 doi:10.1016/j.preteyeres.2005.11.001
- Baehr W, Wu SM, Bird AC, Palczewski K (2003) The retinoid cycle and retina disease. *Vision Research* 43(28):2957-2958 doi:http://dx.doi.org/10.1016/j.visres.2003.10.001
- Ban Y, Rizzolo LJ (2000) Regulation of glucose transporters during development of the retinal pigment epithelium. *Dev Brain Res* 121(1):89-95 doi:Doi 10.1016/S0165-3806(00)00028-6
- Beatty S, Koh H-H, Phil M, Henson D, Boulton M (2000) The Role of Oxidative Stress in the Pathogenesis of Age-Related Macular Degeneration. *Survey of Ophthalmology* 45(2):115-134 doi:http://dx.doi.org/10.1016/S0039-6257(00)00140-5
- Blaug S, Quinn R, Quong J, Jalickee S, Miller SS (2003) Retinal pigment epithelial function: a role for CFTR? *Doc Ophthalmol* 106(1):43-50 doi:Doi 10.1023/A:1022514031645
- Bosl MR, et al. (2001) Male germ cells and photoreceptors, both dependent on close cell-cell interactions, degenerate upon CIC-2Cl(-) channel disruption. *Embo J* 20(6):1289-1299 doi:DOI 10.1093/emboj/20.6.1289
- Brady ST, Siegel GJ, Albers RW, Price DL (2012) *Basic Neurochemistry: Principles of Molecular, Cellular and Medical Neurobiology*. Elsevier Academic Press
- Burnstock G (2007) Purine and pyrimidine receptors. *Cellular and molecular life sciences : CMLS* 64(12):1471-83 doi:10.1007/s00018-007-6497-0
- Campochiaro PA, Jerdon JA, Glaser BM (1986) The extracellular matrix of human retinal pigment epithelial cells in vivo and its synthesis in vitro. *Invest Ophthalmol Vis Sci* 27(11):1615-21
- Collison DJ, Tovell VE, Coombes LJ, Duncan G, Sanderson J (2005) Potentiation of ATP-induced Ca²⁺ mobilisation in human retinal pigment epithelial cells. *Experimental eye research* 80(4):465-475 doi:http://dx.doi.org/10.1016/j.exer.2004.09.009
- Corriden R, Insel PA (2010) Basal release of ATP: an autocrine-paracrine mechanism for cell regulation. *Sci Signal* 3(104):re1 doi:10.1126/scisignal.3104re1
- De La Fuente R, Namkung W, Mills A, Verkman AS (2008) Small-molecule screen identifies inhibitors of a human intestinal calcium-activated chloride channel. *Molecular pharmacology* 73(3):758-68 doi:10.1124/mol.107.043208
- Edelman JL, Miller SS (1991) Epinephrine Stimulates Fluid Absorption across Bovine Retinal-Pigment Epithelium. *Invest Ophth Vis Sci* 32(12):3033-3040
- Eichmann A, Simons M (2012) VEGF signaling inside vascular endothelial cells and beyond. *Current Opinion in Cell Biology* 24(2):188-193 doi:http://dx.doi.org/10.1016/j.ceb.2012.02.002
- El-Tayeb A, Qi A, Muller CE (2006) Synthesis and structure-activity relationships of uracil nucleotide derivatives and analogues as agonists at human P2Y₂, P2Y₄, and P2Y₆ receptors. *Journal of medicinal chemistry* 49(24):7076-87 doi:10.1021/jm060848j
- Eysteinsen T, Hardarson SH, Bragason D, Stefánsson E (2014) Retinal vessel oxygen saturation and vessel diameter in retinitis pigmentosa. *Acta Ophthalmologica:n/a-n/a* doi:10.1111/aos.12359
- Ferrari S, Di Iorio E, Barbaro V, Ponzin D, Sorrentino FS, Parmeggiani F (2011) Retinitis pigmentosa: genes and disease mechanisms. *Current genomics* 12(4):238-49 doi:10.2174/138920211795860107
- Greger R (2000) Role of CFTR in the colon. *Annual review of physiology* 62:467-91 doi:10.1146/annurev.physiol.62.1.467
- Guha S, et al. (2013) Lysosomal alkalization, lipid oxidation, and reduced phagosome clearance triggered by activation of the P2X₇ receptor. *FASEB journal : official publication of the Federation of American Societies for Experimental Biology* 27(11):4500-9 doi:10.1096/fj.13-236166
- Hamann S, et al. (1998) Aquaporins in complex tissues: distribution of aquaporins 1-5 in human and rat eye. *The American journal of physiology* 274(5 Pt 1):C1332-45
- Hughes BA, Takahira M (1996) Inwardly rectifying K⁺ currents in isolated human retinal pigment epithelial cells. *Invest Ophth Vis Sci* 37(6):1125-1139
- Jentsch TJ, Stein V, Weinreich F, Zdebek AA (2002) Molecular structure and physiological function of chloride channels. *Physiological reviews* 82(2):503-68 doi:10.1152/physrev.00029.2001
- Jiang L-H (2012) P2X receptor-mediated ATP purinergic signalling in health and disease. *Cell Health Cytoskeleton* 4:83-101

- Keeling DJ, Taylor AG, Smith PL (1991) Effects of NPPB (5-nitro-2-(3-phenylpropylamino)benzoic acid) on chloride transport in intestinal tissues and the T84 cell line. *Biochimica et biophysica acta* 1115(1):42-8
- Kongsuphol P, Schreiber R, Kraidith K, Kunzelmann K (2011) CFTR induces extracellular acid sensing in *Xenopus* oocytes which activates endogenous Ca^{2+} -activated Cl^{-} conductance. *Pflugers Archiv : European journal of physiology* 462(3):479-87
doi:10.1007/s00424-011-0983-9
- Kramer F, et al. (2000) Mutations in the VMD2 gene are associated with juvenile-onset vitelliform macular dystrophy (Best disease) and adult vitelliform macular dystrophy but not age-related macular degeneration. *European journal of human genetics : EJHG* 8(4):286-92
doi:10.1038/sj.ejhg.5200447
- Loewen ME, Smith NK, Hamilton DL, Grahn BH, Forsyth GW (2003) CLCA protein and chloride transport in canine retinal pigment epithelium. *American journal of physiology Cell physiology* 285(5):C1314-21 doi:10.1152/ajpcell.00210.2003
- Maminishkis A, et al. (2002) The P2Y₂ receptor agonist INS37217 stimulates RPE fluid transport in vitro and retinal reattachment in rat. *Invest Ophthalmol Vis Sci* 43(11):3555-66
- Marieb EN, Hoehn K (2007) *Human anatomy & physiology*, 7th edn. Pearson Benjamin Cummings, San Francisco
- Marmorstein LY, et al. (2006) The light peak of the electroretinogram is dependent on voltage-gated calcium channels and antagonized by bestrophin (best-1). *The Journal of general physiology* 127(5):577-89 doi:10.1085/jgp.200509473
- Mattapallil MJ, et al. (2012) The Rd8 mutation of the *Crb1* gene is present in vendor lines of C57BL/6N mice and embryonic stem cells, and confounds ocular induced mutant phenotypes. *Invest Ophthalmol Vis Sci* 53(6):2921-7 doi:10.1167/iovs.12-9662
- Mitchell CH, Reigada D (2008) Purinergic signalling in the subretinal space: a role in the communication between the retina and the RPE. *Purinergic signalling* 4(2):101-7
doi:10.1007/s11302-007-9054-2
- Peng B, Xiao J, Wang K, So KF, Tipoe GL, Lin B (2014) Suppression of microglial activation is neuroprotective in a mouse model of human retinitis pigmentosa. *The Journal of neuroscience : the official journal of the Society for Neuroscience* 34(24):8139-50
doi:10.1523/JNEUROSCI.5200-13.2014
- Peterson WM, Meggyesy C, Yu K, Miller SS (1997) Extracellular ATP activates calcium signaling, ion, and fluid transport in retinal pigment epithelium. *The Journal of neuroscience : the official journal of the Society for Neuroscience* 17(7):2324-37
- Reichhart N, Strauss O (2014) Ion channels and transporters of the retinal pigment epithelium. *Experimental eye research* 126:27-37 doi:10.1016/j.exer.2014.05.005
- Reigada D, et al. (2005) Degradation of extracellular ATP by the retinal pigment epithelium. *American journal of physiology Cell physiology* 289(3):C617-24 doi:10.1152/ajpcell.00542.2004
- Reigada D, Mitchell CH (2005) Release of ATP from retinal pigment epithelial cells involves both CFTR and vesicular transport. *American journal of physiology Cell physiology* 288(1):C132-40
doi:10.1152/ajpcell.00201.2004
- Ryan JS, Baldrige WH, Kelly ME (1999) Purinergic regulation of cation conductances and intracellular Ca^{2+} in cultured rat retinal pigment epithelial cells. *The Journal of physiology* 520 Pt 3:745-59
- Schultz BD, Singh AK, Devor DC, Bridges RJ (1999) Pharmacology of CFTR chloride channel activity. *Physiological reviews* 79(1 Suppl):S109-44
- Silverthorn DU (2007) *Human Physiology: An Integrated Approach*. Pearson/Benjamin Cummings
- Stevens A, Lowe JS (2005) *Human histology*, 3. edn. Elsevier/Mosby, Philadelphia
- Strauss O (2005) The retinal pigment epithelium in visual function. *Physiological reviews* 85(3):845-81
doi:10.1152/physrev.00021.2004
- Taylor AL, et al. (1999) Epithelial P2X purinergic receptor channel expression and function. *Journal of Clinical Investigation* 104(7):875-884
- Wen H, Hao J, Li SK (2013) Characterization of human sclera barrier properties for transscleral delivery of bevacizumab and ranibizumab. *Journal of pharmaceutical sciences* 102(3):892-903
doi:10.1002/jps.23387
- Wills NK, et al. (2000) Chloride channel expression in cultured human fetal RPE cells: response to oxidative stress. *Invest Ophthalmol Vis Sci* 41(13):4247-55
- Wimmers S, Karl MO, Strauss O (2007) Ion channels in the RPE. *Progress in retinal and eye research* 26(3):263-301 doi:10.1016/j.preteyeres.2006.12.002

- Yang D, Elner SG, Clark AJ, Hughes BA, Petty HR, Elner VM (2011) Activation of P2X receptors induces apoptosis in human retinal pigment epithelium. *Invest Ophthalmol Vis Sci* 52(3):1522-30 doi:10.1167/iops.10-6172
- Young MT, Pelegrin P, Surprenant A (2007) Amino acid residues in the P2X7 receptor that mediate differential sensitivity to ATP and BzATP. *Molecular pharmacology* 71(1):92-100 doi:10.1124/mol.106.030163
- Zhang J, Tuo J, Cao X, Shen D, Li W, Chan CC (2013) Early degeneration of photoreceptor synapse in Ccl2/Cx3cr1-deficient mice on Crb1(rd8) background. *Synapse* 67(8):515-31 doi:10.1002/syn.21674

Appendix

Appendix A license to use laboratory animals for the study



Dr. Þór Eysteinnsson
Lífisfræðistofnun HÍ
Vatnsmýrarvegi 16
101 Reykjavík

TILRAUNADÝRANEFND

Formaður: Halldór Runólfsson, yfirdýralæknir
Sigríður Björnsdóttir, dýralæknir
Jón Kalmannsson, siðfræðingur

Heimilisfang:

Matvælastofnun,
Austurvegi 64, 800 Selfoss,
Sími: 530 4800, Fax: 530 4801
tilraunadyr@mast.is

Selfossi 10.01.2012

Leyfisnúmer: 0112 - 0101-

Levfi fyrir dýratilraun

Umsókn yðar, dagsett 06.09.2011, um leyfi fyrir tilraunina "Þáttur Purine viðtaka í starfsemi sjónhimnu og hlutverk í sjónskynjun", barst tilraunadýranefnd 8. 09. 2011

Umsókn yðar var tekin fyrir á fundi tilraunadýranefndar 9. janúar síðastliðinn. Tilraunadýranefnd telur tilraunina uppfylli ákvæði reglugerðar nr. 279/2002 um dýratilraunir.

Yður er því veitt heimild til að framkvæma tilraunina "Þáttur Purine viðtaka í starfsemi sjónhimnu og hlutverk í sjónskynjun" í 2 ár frá dagsetningu þessa leyfisbréfs eins og henni er lýst í umsókn yðar frá 06.09.2011. Leyfið er veitt að því tilskyldu að þér annist þær tilraunir sem framkvæmdar verða á tilraunadýrunum.

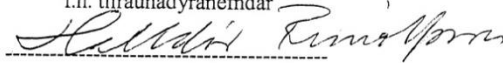
Ef tilraunin veldur dýrunum vanlíðan skal umsvifalaust dregið úr þrautum dýrsins með viðurkenndum deyfilyfjum, eða þau að öðrum kosti aflífuð.

Öll búr þeirra dýra sem notuð verða í þessa tilraun skulu merkt með ofangreindu leyfisnúmeri.

Nefndin minnir yður á að samkvæmt ákvæðum 23. gr. reglugerðar nr. 279/2002 um dýratilraunir, skuluð þér skila skýrslu til tilraunadýranefndar, fyrir 1. febrúar ár hvert, um þær tilraunir sem þér hafið framkvæmt á árinu þar á undan. Afriti skal sent til héraðsdýralæknis Gullbringu- og Kjósarumdæmis. Samkvæmt fyrrnefndri grein reglugerðarinnar er yður einnig skylt að halda dagbók um dýratilraunirnar sem ávallt skulu aðgengilegar eftirlitsaðilum.

Frá og með 27. maí 2003, hefur tilraunadýranefnd heimild frá umhverfisráðuneytinu til að innheimta leyfisgjald fyrir þau leyfi sem nefndin veitir. Fyrir hverja tilraun sem tilraunadýranefnd veitir leyfi fyrir, skal leyfishafi greiða fjárupphæð sem nemur 5000.- krónum og er sú upphæð í samræmi við lög nr. 88/1991 um aukatekjur ríkissjóðs. Yður mun berast í pósti giróseðill frá fjársýslu ríkisins fyrir þessu gjaldi.

Virðingarfyllst,
f.h. tilraunadýranefndar



Halldór Runólfsson
yfirdýralæknir
formaður tilraunadýranefndar